7. Identifying the Occurrence Time of an Impending Mainshock

Abstract. Natural time enables the determination of the occurrence time of an impending major earthquake since it can identify when a complex system approaches a critical point. Considering that the detection of a SES activity signifies that the system enters the critical regime, the small earthquakes that occur (in the region candidate to suffer the mainshock) after the SES detection are analyzed in natural time. It was found that the variance κ_1 of natural time becomes equal to 0.070 (which manifests the approach to the critical point) usually a few days to around one week *before* the mainshock. This, which exhibits spatial as well as magnitude threshold invariance, has been observed to date for *all* major earthquakes that occurred in Greece since the introduction of the natural time concept in 2001 (note that it has been also ascertained in retrospect for the two major earthquakes in Greece during the previous decade, i.e., in the 1990s). For example, the occurrence time of the M_w6.9 earthquake on February 14, 2008, which is the strongest earthquake in Greece during the last 28 years, was announced as imminent on February 10, 2008. The procedure has been also ascertained in the case of the volcanic-seismic swarm activity in 2000 in the Izu island region in Japan as well as of the M_s7.1 Loma Prieta earthquake in California in 1989.

7.1 Determination of the time-window of the impending mainshock by analyzing in natural time the seismicity after the initiation of the SES activity

We first recall (see Eq. (2.75) or Eq. (6.7)) that the relation

$$\Pi(\omega) = \frac{18}{5\omega^2} - \frac{6\cos\omega}{5\omega^2} - \frac{12\sin\omega}{5\omega^3}. \tag{7.1}$$

for $\omega \to 0$, simplifies to

$$\Pi(\omega) \approx 1 - 0.070\omega^2 \tag{7.2}$$

P.A. Varotsos et al., *Natural Time Analysis: The New View of Time: Precursory Seismic Electric Signals, Earthquakes and other Complex Time Series*, Springer Praxis Books, DOI 10.1007/978-3-642-16449-1_7,

which shows that the second-order Taylor expansion coefficient of $\Pi(\omega)$, labeled κ_1, is equal to 0.070. The quantity κ_1 equals (see Eq. (2.37)) to the variance $\langle\chi^2\rangle - \langle\chi\rangle^2$ of natural time χ, i.e.,

$$\kappa_1 = \langle\chi^2\rangle - \langle\chi\rangle^2 = 0.070. \tag{7.3}$$

This has been shown for SES activities (§ 2.4.2) as well as for the time series of avalanches in a number of dynamical models (see Table 8.1), including the "train" Burridge–Knopoff earthquake model (§ 8.2.2) and the Olami–Feder–Christensen earthquake model (§ 8.3.2), when the system approaches the critical point. Furthermore, since it has been observed for several EQs that, when analyzing the seismicity that occurs after the SES activity, the resulting κ_1 value slowly approaches to 0.070 just before the mainshock and abruptly changes to vanishingly small when the main shock occurs, it was proposed (see § 6.2.1) that κ_1 (or $\Pi(\omega)$ for $\omega \to 0$) may be considered as an *order parameter for seismicity* [54].

In addition, we recall that the entropy S in natural time as well as the entropy S_- under time reversal, have been found(see Eq. (4.32)) to obey the following conditions [55, 51, 50] for SES activities

$$S, S_- < S_u. \tag{7.4}$$

These also hold for long-range correlated fBm time series with $\alpha_{DFA} \approx 1$ (see § 3.4.3) as well as for an on–off intermittency model when the critical value is approached from *below* (see § 3.4.4) . Note that it has been suggested that [23] "The Californian earthquakes are long-range correlated according to the persistence of a fractal Gaussian intermittent noise with $H = 1$ known as $1/f$ or pink noise" as well as that [7]: the intermittent criticality model as being more appropriate for earthquakes.

In view of the above and based on our fundamental premise that mainshock occurrence is a critical phenomenon, the conditions (7.1) to (7.3) and (7.4) have been used to study the evolution of seismicity in natural time before a mainshock occurrence. To obtain the order parameter κ_1 or $\Pi(\omega)$ for $\omega \to 0$ (as well as the quantities S and S_-), however, it is necessary to decide the initiation time of seismicity analysis. We decided to start the analysis immediately after the SES initiation since it signals, as mentioned in § 6.2.1, that the system enters the critical stage (recall that the SES emission marks *cooperative* orientation of the electric dipoles and hence the establishment of long-range correlations; see § 1.6.2 and § 2.4.2).

Once a SES activity has been recorded, the area to suffer the mainshock can be estimated, as explained in § 1.3.5, on the basis of the so-called selectivity map of the station at which the SES was recorded and in addition by considering the ratio of the two SES components. Thus, we have in principle some area (see also the discussion in § 7.2.3), labeled A, in which we count the small EQs, e_i , that occur after the initiation of the SES activity. In order to check the spatial invariance of the results, the study was also repeated for a smaller area. This procedure, which for the sake of convenience will be hereafter, called *preliminary* procedure, was used during the period 2001–2008 in a series of publications (e.g., see Refs. [45, 54, 51, 50, 35, 48]) to determine the occurrence time of the impending mainshock by means of the natural time analysis of the seismicity subsequent to a SES activity. Since there has been, however, some room for subjective judgment to identify the approach to critical stage, because the time variation of parameters was traced only on a single subarea, a more objective procedure, which for reasons of brevity will be hereafter

called "*updated*" procedure, has been developed [21], in 2008, and considers the natural time analysis of the seismicity in *all* the possible subareas, instead of a single smaller area, of the larger area under discussion.

7.1.1 The *preliminary* procedure to determine the occurrence time of the impending mainshock

The actual procedure was carried out as follows. We set the natural time zero at the initiation time of the SES activity, and then formed time series of seismic events in natural time for the area A, each time when a small EQ (above a magnitude threshold $M \geq M_{thres}$) occurred; in other words, when the number of the events increased by one. The normalized power spectrum in natural time $\Pi(\omega)$ for $\omega \to 0$ (or the variance κ_1) for each of the time series was computed for the pairs (χ_k, Q_k) and compared with that of Eq. (7.1) for $\omega \in [0, \pi]$. We also calculated the evolution of the quantities S and S_- to ascertain Eq. (7.4) was also satisfied. The actual criteria for recognizing a *true* coincidence of the observed time series with that of critical state were as follows [45, 35, 51, 50, 48]:

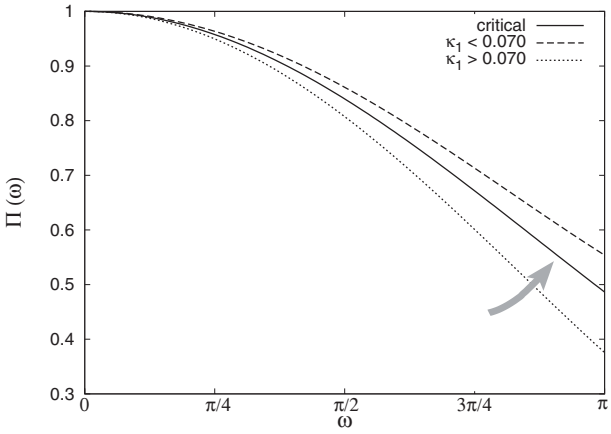

Fig. 7.1 Schematic diagram showing the normalized power spectrum $\Pi(\omega)$ in natural time for $\omega \in [0, \pi]$. Solid line is $\Pi(\omega)$ obtained from Eq. (7.1) which holds for critical stage ($\kappa_1 = 0.070$), whereas two other lines are for $\kappa_1 > 0.070$ and $\kappa_1 < 0.070$. The grey arrow indicates how the $\Pi(\omega)$ curve approaches the critical from below.

First, the 'average' $\langle D \rangle$ distance between the curves of $\Pi(\omega)$ of the evolving seismicity and Eq. (7.1) for $\omega \in [0, \pi]$ should be smaller than 10^{-2} (note that this was regarded as showing that $\langle D \rangle = 0$). This was a practical criterion for stopping calculation.

Second, the final approach of the evolving $\Pi(\omega)$ to that of Eq. (7.1) must be by approaching from *below* as shown by the grey arrow in Fig. 7.1. This alternatively means that before major EQs, the κ_1 value gradually changes with time and *finally* approaches from *above* that of the critical state ($\kappa_1 = 0.070$, see Eq. (7.3)). This rule was found empirically [45].

Third, both values S and S_- should be smaller than $S_u (= 0.0966)$ at the coincidence (see Eq. (7.4)).

Finally and fourth, since the process concerned is supposed to be self-similar (critical dynamics), the time of the occurrence of the *true* coincidence should not vary, in principle, upon changing (within reasonable limits) the magnitude threshold M_{thres} and the size of area A.

We clarify, however, that if higher magnitude threshold is used, the description of the real situation approaching criticality is expected to become less accurate due to *'coarse graining'* [43, 49] since the number of events is finite.

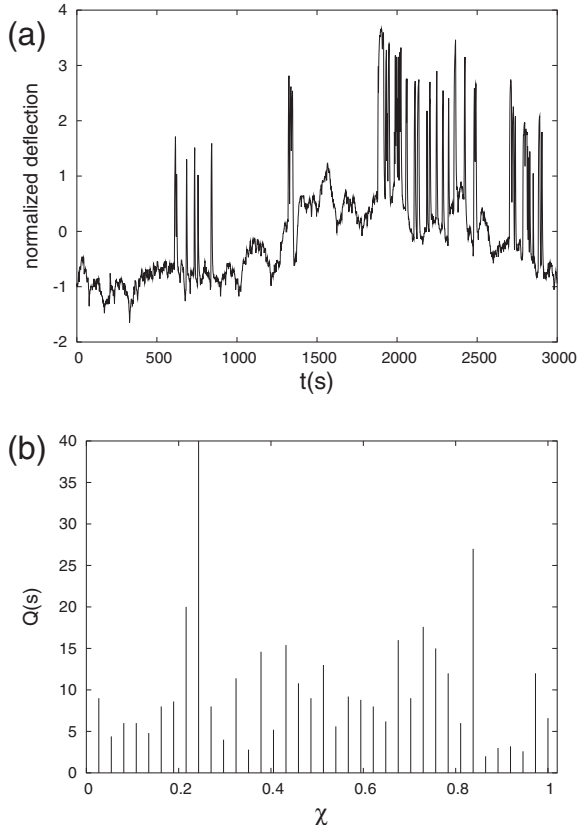

Fig. 7.2 (a) A SES activity recorded on February 13, 2006 at PAT station(sampling rate $f_{exp} = 1$ Hz). The actual electric field E of the SES pulses is 6 mV/km (see Ref. [49]), but here the signal is presented in normalized units, i.e., by subtracting the mean value and dividing by the standard deviation. (b) How the SES activity in (a) is read in natural time. Taken from Ref. [50].

It has been observed [45, 35, 51, 50, 48] that the aforementioned *true* coincidence appears usually a few days (up to around one week) *before* the occurrence of the mainshock. As an example, we report a SES activity recorded at a station located in central Greece (close to Patras city, PAT; see Fig. 1.2) on February 13, 2006. It is depicted in Fig. 7.2(a) and comprises 37 pulses, the durations Q_k of which vary between 1 s and 40 s (see Fig. 7.2(b)). Beyond the application of the four criteria of Section 1.2, a natural time

analysis of this SES activity (labeled PAT in Table 4.6) was made which led [50] to the following values: $\kappa_1 = 0.072 \pm 0.002$, $S = 0.080 \pm 0.002$, $S_- = 0.078 \pm 0.002$ which obey the conditions (4.38) and (4.39), i.e., $\kappa_1 \approx 0.070$ and $S, S_- < S_u$, that have to be obeyed for SES activities. In addition, the Detrended Fluctuation Analysis (DFA) (§ 1.4.2) in natural time of this SES activity, resulted in an exponent $\alpha = 1.07 \pm 0.36$, which agrees with the finding $\alpha \approx 1$ in several other SES activities (see § 4.4.2 and Eq. (4.42)). If we repeat the computation by *shuffling* the durations Q_k randomly (and hence their distribution is conserved), the corresponding quantities, designated by adding a subscript "shuf", have the following values: $\kappa_{1,shuf} \approx \kappa_u$ and $S_{shuf} \approx S_{-,shuf} \approx S_u$. This points to the conclusion that the self-similarity of SES activities results from the process's memory only (see § 4.7.1 and § 2.5.5). All these results showing that the signal recorded on February 13, 2006, is a true SES activity were submitted [50] for publication on February 25, 2006 (see Table 7.1). Actually, on April 3, 2006, a strong seismic activity started with an earthquake of magnitude $M_s(\text{ATH}) = 5.3$ and lasted until April 19, 2006 with earthquakes of magnitude up to 5.9 in a region 80 to 100 km west of PAT station, i.e., around 37.6°N 20.9°E (see also table I of Ref. [49]). We will now explain how the occurrence time of the initiation of this earthquake activity has been specified [49] by following the *preliminary* procedure:

First, after the recording of this SES activity, the area to suffer the impending mainshock was estimated as follows: We considered that the epicenters of the EQs that have been preceded, up to that time, by SES activities at PAT station lie approximately within the area $\text{N}_{37.5}^{38.6}\,\text{E}_{19.8}^{23.3}$, i.e., this was the selectivity map (§ 1.3.4) of PAT station. Then, by using the additional information of the ratio of the two SES components (§ 1.3.5), we selected from the selectivity map the region A: $\text{N}_{37.6}^{38.6}\,\text{E}_{20.9}^{22.6}$ as candidate that might have emitted the SES activity under discussion.

Second, we now study in natural time the seismicity that evolved after the recording of the relevant SES activity at PAT, thus we put natural time zero for seismicity at the initiation time of this SES activity, i.e., at 19:04 UT on February 13, 2006. The study is made in the areas A: $\text{N}_{37.55}^{38.64}\,\text{E}_{20.85}^{22.64}$ as well as in its smaller area B: $\text{N}_{37.55}^{38.34}\,\text{E}_{20.85}^{22.15}$. We now form time series of seismic events in natural time for various time windows as the number N of consecutive (small) EQs increases. We then compute the normalized power spectrum of seismicity in natural time $\Pi(\phi)$ (for $\phi \to 0$, e.g. $\phi \in [0, 0.5]$) for each of the time windows. We clarify that the seismic moment M_0 was estimated from the relation [5] $\log_{10}(M_0) = 1.5 M_w + \text{const.}$ by using $M_w = 1.09 M_L - 0.21$, i.e., the least-squares fit proposed in Ref. [19], and the values of the local magnitude M_L were taken from the GI-NOA catalog. In short, the relation $\log_{10}(M_0) = 1.64 M_L + \text{const.}$ has been used. Excerpts of the results of these computations which refer to the values deduced during the period March 27 to April 1, 2006, are depicted in red in Fig. 7.3. In this figure, Fig. 7.3(a) corresponds to the area A with magnitude threshold $M_{thres} = 3.0$ (defined by means of the local magnitude M_L and of the 'duration' magnitude M_D), while Fig. 7.3(b) to the area B with $M_{thres} = 2.8$. In the same figure, we plot in blue the normalized power spectrum obeying Eq. (7.1). The date and the time of the occurrence of each small earthquake (with magnitude exceeding (or equal to) the aforementioned threshold) that occurred in each of the areas A and B, is also written in red in each panel.

Table 7.1 All EQs with $M_s(\text{ATH}) \geq 6.0$ within $\text{N}_{36}^{41}\,\text{E}_{19}^{27}$ since 2001 along with the relevant SES activities. The cases in parentheses refer to EQs for which the expected magnitude (on the basis of the SES amplitude) was $M_s(\text{ATH}) \approx 6.0$, but the actual magnitude turned out to be somewhat smaller. The last column gives, in each case, the relevant documentation publicized *before* the mainshock occurrence, when available. The EQs grouped together refer to almost the same epicentral location.

EQ			Related SES activities		
Date	Epicenter	Magnitude	Station	Date	Publication
D/M/Y	°N–°E	M_s(ATH)– M_w(USGS)		D/M/Y	
26/7/2001	39.05–24.35	5.8–6.5	VOL	17/3/2001	Ref. [41] submitted on 25 March 2001
14/8/2003	38.79–20.56	6.4–6.2	PIR	8/8/2003	Ref. [35]
31/1/2005	37.41–20.11	6.2–5.7	PIR	17/10/2004	Ref. [52]
17/10/2005	38.13–26.59	6.0–5.5	MYT	21/3 and 23/3/2005	Ref. [51] submitted on 16 April 2005 and Ref. [43]
(17/10/2005	38.14–26.59	5.9–5.8	MYT	21/3 and 23/3/2005	Ref. [51] submitted on 16 April 2005 and Ref. [43])
20/10/2005	38.15–26.63	6.1–5.9	MYT	21/3 and 23/3/2005	Ref. [51] submitted on 16 April 2005 and Ref. [43]
18/10/2005	37.58–20.86	6.1–5.7	PIR	17/9/2005	Ref. [42] submitted on 22 October 2005 and Ref. [43]
8/1/2006	36.21–23.41	6.9–6.7	PIR	17/9/2005	Ref. [42] submitted on 22 October 2005 and Ref. [43]
(3/4/2006	37.59–20.95	5.3–5.0	PAT	13/2/2006	arXiV:0602603v1 [25 February 2006] and Ref. [50])
(4/4/2006	37.58–20.93	5.7–5.3	PAT	13/2/2006	arXiV:0602603v1 [25 February 2006] and Ref. [50])
(11/4/2006	37.64–20.92	5.7–5.4	PAT	13/2/2006	arXiV:0602603v1 [25 February 2006] and Ref. [50])
(11/4/2006	37.68–20.91	5.9–5.5	PAT	13/2/2006	arXiV:0602603v1 [25 February 2006] and Ref. [50])
(12/4/2006	37.61–20.95	5.9–5.6	PAT	13/2/2006	arXiV:0602603v1 [25 February 2006] and Ref. [50])
25/3/2007	38.34–20.42	6.0–5.7	PAT	8/2/2007	arXiv:0703683v1 [26 March 2007]
(29/6/2007	39.25–20.26	5.7–5.2	PAT	23 and 24/4/2007	arXiv:0703683v5 [15 May 2007])
6/1/2008	37.11–22.78	6.6–6.2	PAT	7/11/2007	arXiv:0711.3766v1 [23 November 2007] and Ref. [21]
14/2/2008	36.50–21.78	6.7–6.9	PIR	14/1/2008 and 21-26/1/2008	arXiv:0711.3766v3 [1 February 2008] and Ref. [21]
14/2/2008	36.22–21.75	6.6–6.5	PIR	14/1/2008 and 21-26/1/2008	arXiv:0711.3766v3 [1 February 2008] and Ref. [21]
20/2/2008	36.18–21.72	6.5–6.2	PIR	14/1/2008 and 21-26/1/2008	arXiv:0711.3766v3 [1 February 2008] and Ref. [21]
8/6/2008	37.98–21.51	7.0–6.4	PIR	29/2-2/3/2008	arXiv:0802.3329v4 [29 May 2008] and Ref. [21]
21/6/2008	36.03–21.83	6.0–5.6	PIR	5/6/2008	
14/10/2008	38.85–23.62	6.1–5.2	missed		
(13/12/2008	38.72–22.57	5.7–5.2	PAT	9/10/2008	arXiv:0711.3766v5 [7 December 2008])
16/2/2009	37.13–20.78	6.0–5.5	PIR	12/12/2008	arXiv:0707.3074v3 [5 February 2009] and Ref. [47]
3/11/2009	37.39–20.35	6.1–5.8	PIR	24/10/2009	–
(18/1/2010	38.41–21.95	5.7–5.5	PAT	24/10/2009	arXiV:0904.2465v8 and v9[14 and 27 November 2009])
(22/1/2010	38.42–21.97	5.6–5.2	PAT	11/11/2009	arXiV:0904.2465v8 and v9[14 and 27 November 2009])
(9/3/2010	38.87–23.65	5.6–	LAM	27-30/12/2009	arXiV:1003.1383v1 [6 March 2010])

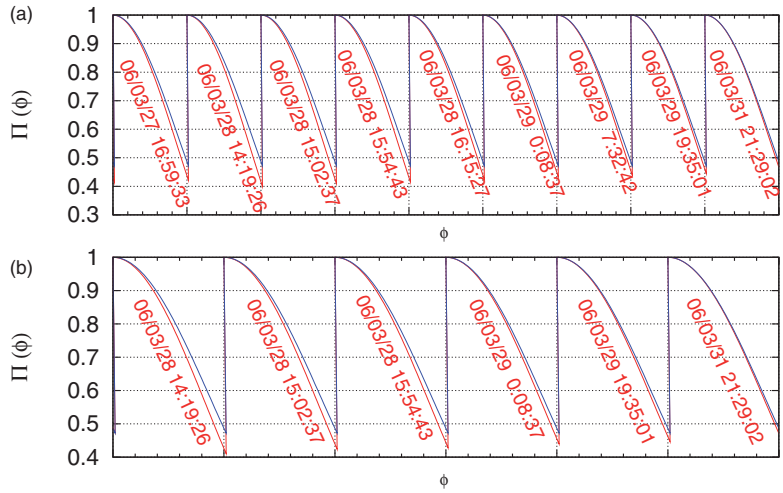

Fig. 7.3 The normalized power spectrum(red) $\Pi(\phi)$ of seismicity as it evolves event by event (whose date and time of occurrence are written in each panel) after the initiation of the SES activity on February 13, 2006. The two excerpts presented here refer to the period March 27 to March 31, 2006, and correspond to: (a) the area A with $M_{thres} = 3.0$ and (b) the area B with $M_{thres} = 2.8$. In each case the spectrum for small ϕ values, e.g. $\phi \in [0, 0.5]$ (for the reasons discussed in Section 2.4) is depicted (separated by the vertical dotted lines), whereas the $\Pi(\phi)$ of Eq. (7.1) is depicted by blue color. The minor horizontal ticks for ϕ are marked every 0.1. Taken from Ref. [49].

An inspection of Fig. 7.3 reveals that the red line approaches the blue line as N increases and a *coincidence* occurs at the last small event which had $M_L = 3.0$ and occurred at 21:29 UT on March 31, 2006, i.e., roughly two days before the first strong EQ (00:50 UT on April 3, 2006). To ensure that this coincidence is a *true* one, we also calculate the evolution of the quantities κ_1, S and S_- and the results are depicted in Fig. 7.4 for both magnitude thresholds 2.8 and 3.0 for each of the areas A and B.

We now examine whether the aforementioned criteria for a coincidence to be considered as *true* are obeyed: First, concerning the 'average' distance $\langle D \rangle$ see Fig. 7.5, where we plot $\langle D \rangle$ versus the conventional time for the aforementioned two areas and the two magnitude thresholds (hence four combinations were studied in total). In order to better visualize the details of this figure, its four consecutive segments are enlarged and separately depicted in Fig. 7.6(a) to (d). Note that in Fig. 7.5 or Fig. 7.6(d), upon the occurrence of the aforementioned last small event of March 31, 2006, in both areas A and B and both magnitude thresholds (i.e., $M_{thres} = 2.8$ and 3.0) their $\langle D \rangle$ values become smaller than 10^{-2}. Second, a few events *before* the coincidence leading to the strong EQ, the evolving $\Pi(\phi)$ has been found to approach that of Eq. (7.1), i.e., the blue one in Fig. 7.3, from *below* (note that this reflects that during this approach the κ_1 value decreases as the number of events increases see Fig. 7.4(a)). In addition, both values S and S_- are smaller than S_u at the coincidence; see Fig. 7.4(b) and 7.4(c), respectively. Finally, since the process concerned is self-similar

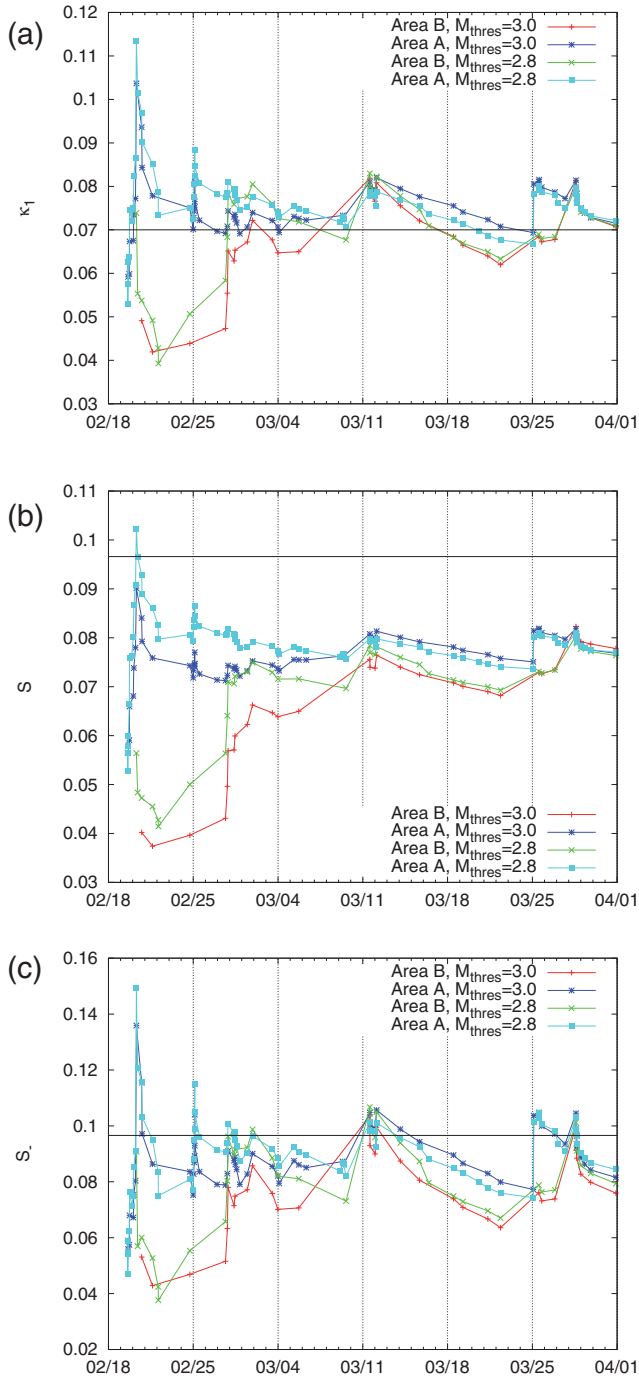

Fig. 7.4 Evolution of the quantities κ_1, S and S_- for seismicity after the initiation of the SES activity on February 13, 2006, depicted in Fig. 7.2(a). They are shown in (a), (b) and (c), respectively for two magnitude thresholds, i.e., $M \geq 2.8$ and $M \geq 3.0$, for both areas A and B. After the event at 14:19 UT of March 28, 2006 the four curves (corresponding to the four combinations, i.e., resulting from the two areas and the two magnitude thresholds) *almost collapse on the same curve*. This points to the *scale invariance* when approaching the critical point (see the text). Taken from Ref. [49].

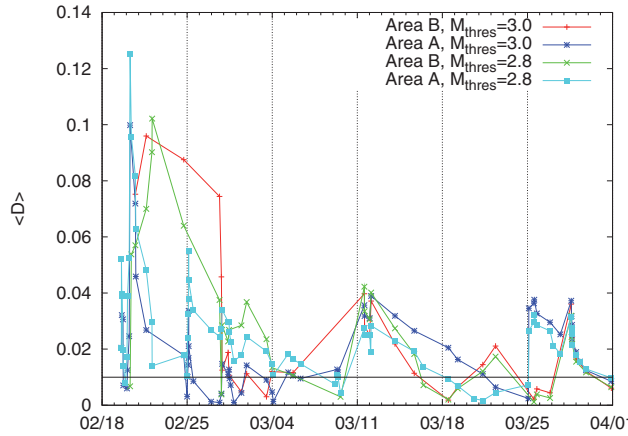

Fig. 7.5 The average distance $\langle D \rangle$ versus the conventional time. The calculation of $\langle D \rangle$ is made upon the occurrence of every consecutive earthquake when starting the calculation after the SES activity of February 13, 2006 (depicted in Fig. 7.2(a)), for each of the two areas A and B by considering two magnitude thresholds 2.8 and 3.0. Taken from Ref. [49].

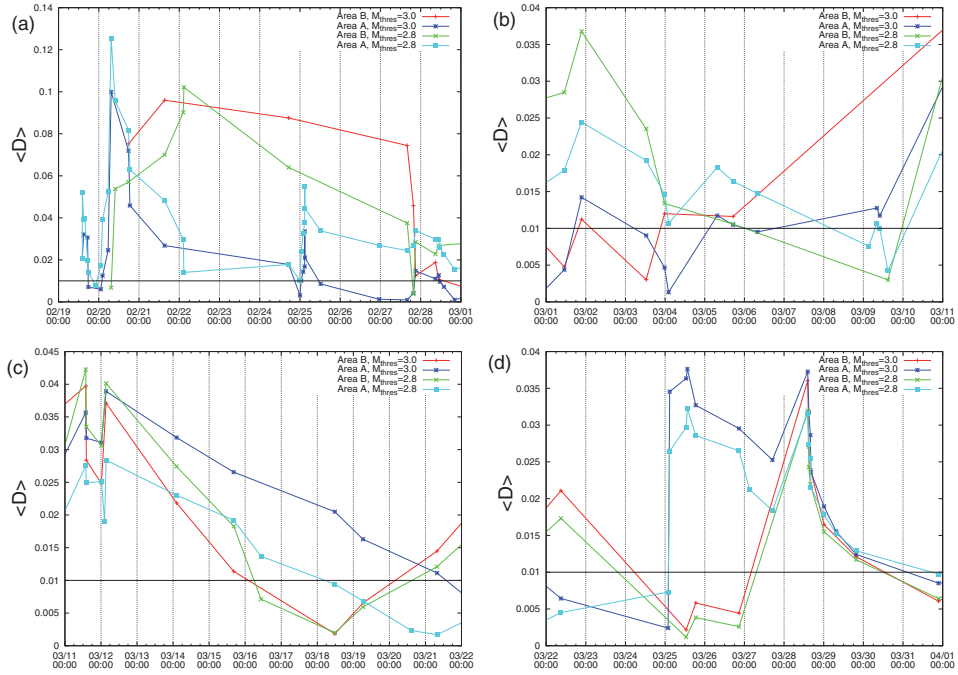

Fig. 7.6 Four consecutive segments of Fig. 7.5. Note that in (d), after 14:19 UT of March 28, 2006 the four curves (corresponding to the four combinations resulting from the two areas and the two magnitude thresholds) *almost collapse on the same curve*. This points to the *scale invariance* when approaching the critical point (see the text). Taken from Ref. [49].

(*critical* dynamics), the occurrence time of the (true) coincidence should *not* change, in principle, upon changing either the (surrounding) area or the magnitude threshold used in the calculation. This was actually checked in this example since we considered two areas and two magnitude thresholds. Hence, this coincidence can be considered as *true*, while other coincidences that occurred earlier (i.e., before March 31, 2006) have been found *not to be true ones* since they violate one or more of the aforementioned conditions. Let us briefly summarize:

The occurrence time of the initiation of the strong seismic activity, that lasted from April 3 to April 19, 2006 at an epicentral region 80 to 100 km west of PAT, has been specified within a narrow range around 2 days. This is so, because the normalized power spectrum in natural time of the evolving seismicity after the SES activity of February 13, 2006, collapses on the one expected for critical dynamics at 21:29 UT on March 31, 2006, i.e., almost two days *before* the occurrence time of the 5.3 earthquake of April 3, 2006, obeying the conditions for a *true* coincidence.

Additional examples for the *preliminary* procedure will be presented in § 7.2.1 and § 7.2.4.

7.1.2 The *updated* procedure to determine the occurrence time of the impending mainshock

The basic idea behind the new approach suggested in Ref. [21] is the following. When area A reaches criticality, one expects in general that all its subareas have also reached criticality simultaneously. At that time, therefore, the evolution of seismicity in each of these subareas is expected to result in κ_1 value close to 0.070. Assuming equi-partition of probability among the subareas, the distribution of the κ_1 values of all subareas should be peaked at around 0.070 exhibiting magnitude threshold invariance. Before the criticality is reached, the κ_1 values will *not* show such a behavior.

We recall that, as mentioned above in Section 7.1, once a SES activity has been recorded, we identify in principle an area, labeled A, in which we count the small EQs, e_i, that occur after the initiation of the SES activity. Each EQ e_i is characterized by its epicentral location $\mathbf{x}(e_i)$, the conventional time of its occurrence $t(e_i)$, and its magnitude $\mathrm{M}(e_i)$ or the equivalent seismic moment $M_0(e_i)$. The index $i = 1, 2, \ldots$ increases by one each time a new EQ with M larger or equal to some threshold M_{thres} occurs within the area A. Thus, a set of events denoted as $A_{M_{thres}} = \{e_i\colon\ \mathbf{x}(e_i) \in \mathrm{A},\ \mathrm{M}(e_i) \geq M_{thres}\}$ is formed each time until the mainshock occurs. Here, the number of EQs in $A_{M_{thres}}$ is denoted by $|A_{M_{thres}}|$. Since, in forming $A_{M_{thres}}$, we place the EQs in sequence of their occurrence time, $A_{M_{thres}}$ is a *time-ordered* set.

In practice, in order to check whether criticality as described above has been approached at the occurrence of a new event i within the predicted area A, we should construct all the possible proper subsets of $A_{M_{thres}}$ that *necessarily* include the event i and examine whether their κ_1 values reveal a probability distribution peaked at 0.070. A subset is qualified as a

proper subset ($P_{M_{thres}}$) *iff* it includes all EQs that took place inside its corresponding rectangular subarea denoted by $R(P_{M_{thres}})$. This is a simplification because other geometries, e.g., circular, could be also envisaged. It is worthwhile to clarify, however, that even in the frame of this simplification:

The accuracy in the determination of the epicentral coordinates of the EQs involved in the computation, may somewhat affect – as intuitively expected – the results as it will be further commented on in § 7.2.5.1.

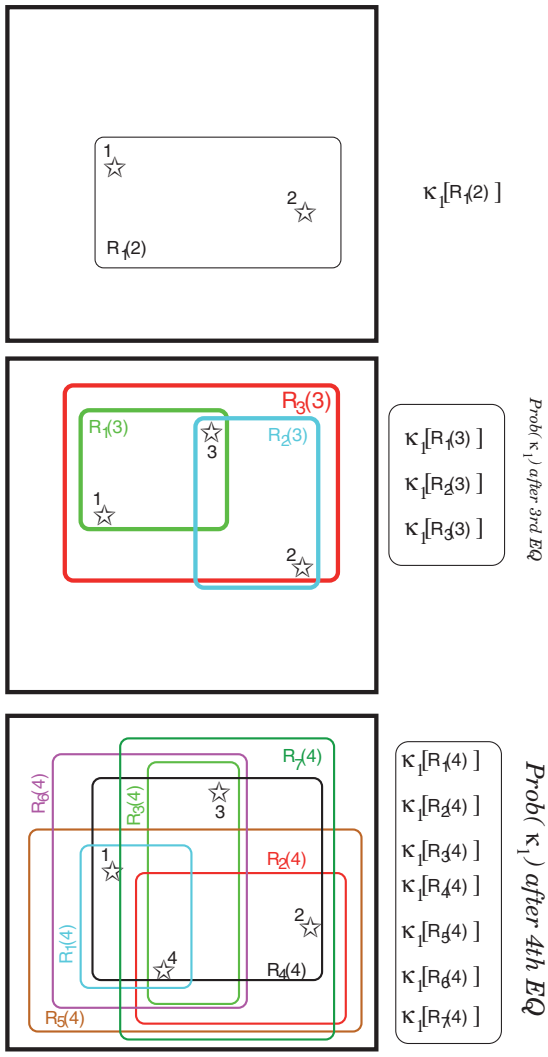

Fig. 7.7 The area A (thick black rectangle) and its rectangular subareas $R_j(i)$, corresponding to the proper subsets immediately after the occurrence of the second EQ "2" (upper panel), the third EQ "3" (middle panel) and the fourth EQ "4" (bottom panel). The location of each EQ is shown by an open star. Right column shows the κ_1 values that can be obtained for each subarea. Taken from Ref. [21].

Let us now consider the schematic example shown in Fig. 7.7, in which four EQs have occurred (area A is indicated by a black line rectangle in each panel) in a sequence indicated by the numbers $i = 1,2,3$ and 4. Colored rectangles depict proper subareas $R(P_{M_{thres}}) = R_j(i)$ just after the occurrence of each EQ. Figure 7.7 shows that the number of subareas j increases by an integer larger than or equal to one, when a new EQ occurs. For each of these proper subsets (which form the $\varepsilon[A_{M_{thres}}]$ ensemble at each time instant), one can compute the κ_1 values and then construct their distribution denoted by $\text{Prob}(\kappa_1)$ hereafter. Just after the occurrence of the second event a single proper subset can be defined, thus only $\kappa_1[R_1(2)]$ is available. Later, just after the occurrence of the third event, three proper subsets of $A_{M_{thres}}$ can be defined as shown in Fig. 7.7. Recall that the necessary condition for a proper subset at a given time instant is that it includes the last event (the third EQ in this case). Therefore, $\kappa_1[R_1(2)]$ obtained before the third event is not included for the construction of the distribution $\text{Prob}(\kappa_1)$ at the instant of the third event. By the same token, after the occurrence of the fourth event, seven proper subsets result. Thus, we can now calculate κ_1 for each of these 7 subsets and construct the $\text{Prob}(\kappa_1)$ versus κ_1 graph to examine whether it maximizes at $\kappa_1 \approx 0.070$ (i.e., if it obeys Eq. (7.3)). In actual cases, the number of EQs, depending on the threshold magnitude, are usually tens to a few hundreds and the number of subareas varies from hundreds up to a few tens of thousands.

In the new approach, the κ_1 values of all these subareas and the largest area A, are treated on *equal* footing, which reflects that the adopted largest area A may be a proper subarea of an even larger area in which the mainshock actually occurs. This is a useful notion when the selectivity map of the concerned station is incomplete or a portion of it is adopted for some reason as in the case of the M_w6.4 EQ on June 8, 2008 (see Table 7.1), that will be discussed later in § 7.2.6.

By summarizing, upon the recording of a SES activity, one can estimate (through the procedure explained in § 1.3.5) an area A within which the impending mainshock is expected to occur. Analyzing in natural time the subsequent seismicity (as it evolves event by event) in *all* the possible subareas of A, the probability density function of κ_1 is obtained until it maximizes at $\kappa_1 \approx 0.070$ exhibiting also magnitude threshold invariance. This usually occurs a few days to around one week *before* the mainshock, thus it enables the prediction of the occurrence time of major EQs with time window of the order of a week or so. Examples of this procedure will be presented in § 7.2.2, § 7.2.3, § 7.2.5 and § 7.2.6.

Note also that, as shown later in § 8.4.3, in the mean field case of a *growing* sandpile (§ 8.4.2) even when studying a *single* realization and select random subseries of the process described by Eq. (8.21) to be analyzed in natural time, the pdf deduced for κ_1 maximizes at $\kappa_1 \approx 0.070$; see Fig. 8.17.

7.2 What happened before all earthquakes in Greece with $M_s(ATH) = 6.0$ or larger since 2001. The cases of the major earthquakes with magnitude $M_w 6.4$ or larger since 1995

Since the introduction of *natural time* [45] in 2001 a number of earthquakes (EQs) with magnitude $M_w = 6.0$ or larger occurred in Greece. In this Section, we report what was observed before these EQs, which are included in Table 7.1 (note that predictions of earlier EQs – which have been undoubtedly shown to clearly outperform chance in a debate published in a Special Issue of Geophysical Research Letters, i.e., Vol. 23, No. 11, May 27, 1996, under the title: Debate on "VAN" – were compiled in Ref. [35]). Particular attention is focused on the five major EQs (see Fig. 7.8) with $M_w \geq 6.4$, i.e., the $M_w 6.5$ at 39.05°N 24.35°E on July 26, 2001, the $M_w 6.7$ at 36.21°N 23.41°E on January 8, 2006, the $M_w 6.9$ at 36.50°N 21.78°E on February 14, 2008, the $M_w 6.5$ at 36.22°N 21.75°E on February 14, 2008, and the $M_w 6.4$ at 37.98°N 21.51°E on June 8, 2008 (note that M_w is taken from [26]). In addition, our attention here is focused on the two major EQs with $M_w > 6.4$ of the previous decade (which are *also* plotted in Fig. 7.8), i.e., the $M_w 6.6$ at 40.14°N 21.67°E on May 13, 1995 and the $M_w 6.5$ at 38.4°N 22.3°E on June 15, 1995, the data of which have been analyzed in natural time in retrospect.

During the last fifteen year period, in accordance with the recommendation of the European Advisory Committee for earthquake prediction of the Council of Europe (see p. 101 of Ref. [35]), the following policy was adopted: *if* the expected EQ magnitude M_s(ATH) estimated from the amplitude of the SES activity was larger than (or equal to) 6.0, quick report on the relevant information was submitted to international journals (e.g., see Refs. [52, 51, 50]) *before* the EQ occurrence. The symbol M_s(ATH) stands for the magnitude defined by

$$M_s(\text{ATH}) = M_L + 0.5, \tag{7.5}$$

where M_L denotes the local magnitude reported by GI-NOA (www.gein.noa.gr/services/monthly-list.html).

In Table 7.1, we include *all* EQs with $M_s(\text{ATH}) \geq 6.0$ that occurred in Greece within the area $\text{N}_{36}^{41}\,\text{E}_{19}^{27}$ since 2001. In addition, this Table also includes in parentheses the data for the cases in which the expected magnitude (documented on the basis of the SES amplitude) was $M_s(\text{ATH}) \approx 6.0$, but the actual EQ magnitude turned out to be somewhat smaller. For each EQ, we tabulate the date and the station at which the relevant SES activity was recorded along with the publication at which this preseismic information was documented. For the reader's convenience, we also give the submission date of each publication in cases where this documentation was made *before* the EQ occurrence. We emphasize that, in this documentation, it has been confirmed that the SES activity reported in each case, was classified as such since it obeys *both* the criteria described in Section 1.2 as well as the criteria in natural time summarized in Section 4.10.

In § 7.2.1 to § 7.2.6, we restrict ourselves to the description on what happened before the major earthquakes in Greece with magnitude $M_w \geq 6.4$ since 1995.

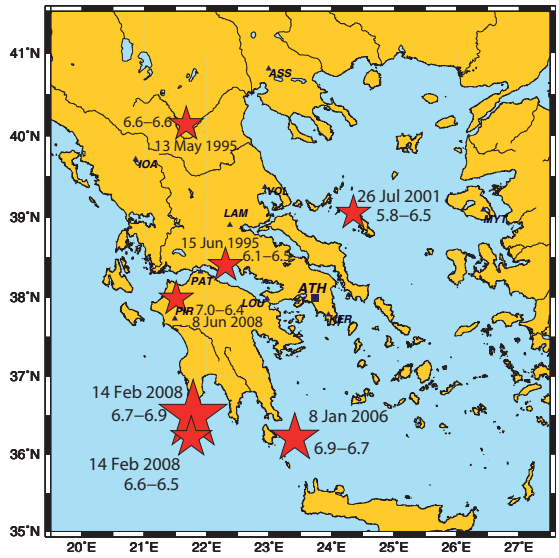

Fig. 7.8 Map showing the location of the VAN stations (triangles) operating in Greece. The location of the central station GLY (which is a suburb of Athens, ATH, rectangle), to which the data of all stations are transferred telemetrically in real time is also shown. The epicenters of the five major EQs with $M_w \geq 6.4$ since 2001(see Table 7.1) along with the two ones in 1995 are indicated by red stars.

7.2.1 The major Grevena-Kozani M_w6.6 earthquake on May 13, 1995

An International Workshop was held by the Royal Society (London, May 11–12, 1995, e.g., see Lighthill [12, 13]) under the title: "A critical review of VAN" just before the occurrence of the M_w6.6 earthquake in Greece on May 13, 1995. This EQ was highly unexpected, because it occurred in an "aseismic" area. The relevant prediction had been forwarded to the chairman of the Workshop (Sir James Lighthill) well in advance (see below). Furthermore, one week after the Workshop, another prediction was sent to the chairman that was related with the catastrophic M_w6.5 Eratini-Egion earthquake of June 15, 1995, which will be discussed in § 7.2.2. These two EQs were the largest events that occurred during 1983–1995 in Greece and their predictions, which attracted a strong interest in the international literature (e.g., Masood [15, 14], Kerr [8], Monastersky [16]), can be found in the Proceedings of the Workshop published several months later (see Varotsos et al. [39]; copies of these predictions are also reproduced here). The chairman included the following conclusion in the Proceedings [13]:

"The earthquakes occurring after the meeting (on 13 May in northern Greece and on 15 June in Egion, which were the two largest in Greece for over a decade) are carefully related to the corresponding VAN predictions (those received by myself, for example – along with other interested scientists – on 2 May and on 20 May 1995). It is noteworthy that the distinguished seismologist, Professor H. Kanamori, was influenced partly by these events, as well as by the proceedings of the review meeting (which he had attended in an initially neutral spirit), to give the views he has expressed above in 'A seismologist looks at VAN', suggesting that for the larger earthquakes in Greece the VAN group appears to have usefully identified SES precursors."

(a)

April 30, 1995

RECENT SEISMIC ELECTRIC SIGNAL ACTIVITIES IN GREECE

by

P. Varotsos and M. Lazaridou

Dept. of Physics, University of Athens, Greece

Abstract: *Three seismic electric signal activities were recently recorded at IOA station. They might indicate that a pronounced series of earthquakes will occur in Greece with M_s≈6.0 units.*

The most catastrophic earthquake (EQ) in Greece during the last eight years seriously damaged the village of Vartholomio on October 16, 1988. The epicenter was at 37.90°N, 20.96°E with a surface wave magnitude (according to the National Observatory of Athens) M_s(ATH)=6.0. It was preceded by a M_s(ATH)=5.5 EQ on Sept. 22, 1988 at 37.99°N, 21.11°E, which destroyed Killini harbour. The prediction of these EQs was publicly announced by Haroun Tazieff (through AFP and Antenne 2 of the French television) after the receipt of related telegrams sent by the first author. Three seismic electrical signals (SES) activities were recorded on Aug. 31, Sept. 29 and Oct. 3, 1988 (at IOA station, located in northwestern Greece) which were extensively discussed by Varotsos and Lazaridou (1991) and by Varotsos et al (1993).

On April 6, 1995, a SES activity was recorded at IOA station with characteristics (polarity, form, etc.) almost similar to those of the aforementioned activities on Sept. 29 and Oct. 3, 1988, but with a smaller amplitude. By following the procedure described by Varotsos and Lazaridou (1991) we concluded that a seismic activity is expected with M_s(ATH)≈5.0 units at an epicenter 200 km west of Athens. This information was sent on April 7, 1995 to the Greek authorities and to 29 Institutes abroad. In the meantime, however, two new SES electrical activities were recorded (on 18 and 19 April, 1995) at IOA station (see Fig. 1) that have comparable amplitudes and almost the same characteristics with those of Sept. 29 and Oct. 3, 1988. Therefore a M_s(ATH)≈6.0 EQ might occur close to the aforementioned Vartholomio area. An alternative solution is M_s(ATH)≈5.5 - 6.0 with an epicenter a few tens of km NW from IOA. Note that the latter solution seems to be more compatible with the experimental fact that ΔV/L differs between the two long dipoles at IOA having unequal lengths (case of nearby source). The two alternative candidates are shown in Fig. 2. The time evolution of the current activity might follow the same time chart as in Fig. 22 of Varotsos et al (1993).

References

Varotsos P. And Lazaridou M. 1991. "Latest aspects of earthquake prediction in Greece based on seismic electric signals I". Tectonophysics 188, 321-347.

Varotsos P., Alexopoulos K. And Lazaridou M. 1993. "Latest aspects of earthquake prediction in Greece based on seismic electric signals II". Tectonophysics 224, 1-37.

(b)

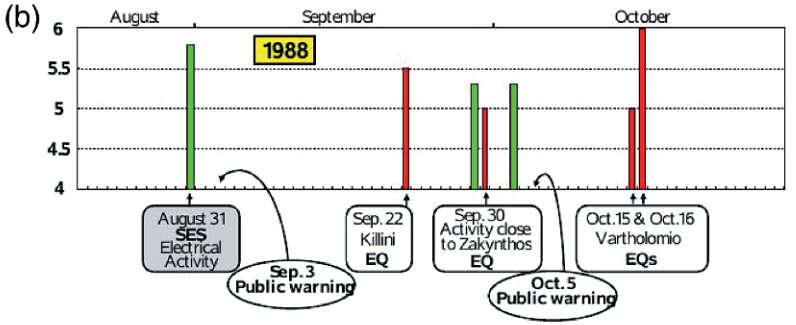

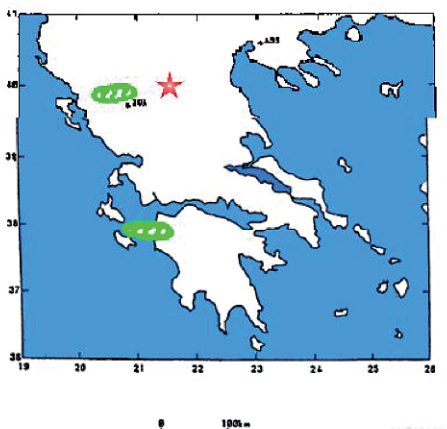

b. Fig. 2. : The two alternative epicenters.

Fig. 7.9 The prediction issued on April 30, 1995, related to the M_w6.6 EQ that occurred on May 13, 1995. A third page was also attached, which was just a copy of the recordings of the SES activities at IOA. For the convenience of the reader, the actual epicenter has been added on the prediction map with a red star.

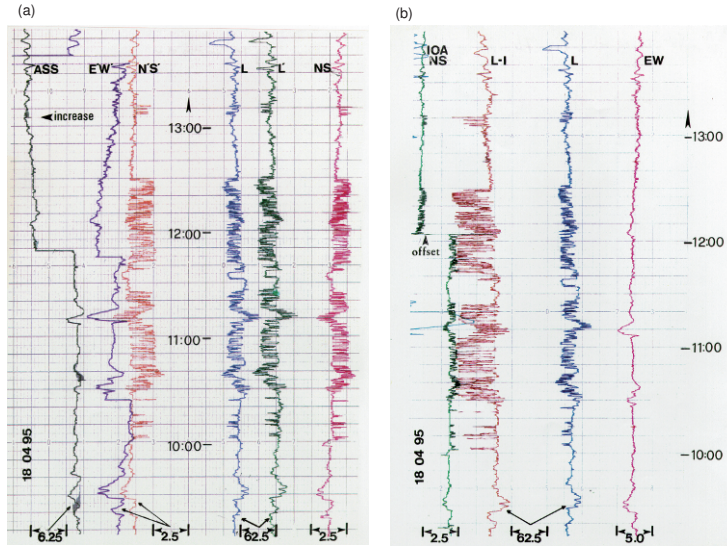

Fig. 7.10 SES activity recorded at IOA on April 18, 1995 (raw data collected by the real-time telemetric network; the scales are in mV). All dipoles are installed at IOA (see the text), except the one labeled ASS (given to distinguish the MT disturbances). The arrow labeled "increase" indicates the direction of increasing ΔV measured in mV. Taken from Ref. [37].

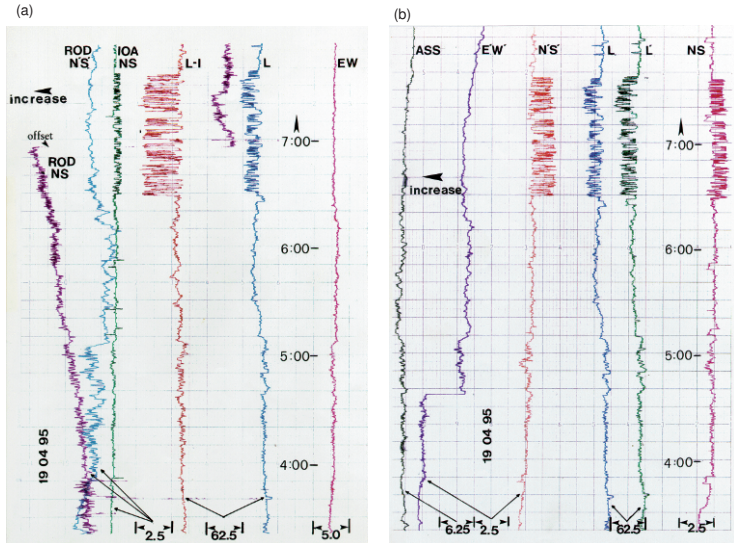

Fig. 7.11 SES activity at IOA on April 19, 1995. They are photocopies from the recordings at the central station (GLY) of the real-time telemetric network. All channels correspond to IOA, except those labeled ROD or ASS, which refer to other stations. The arrow, labeled "increase", indicates the direction of increasing value of ΔV (e.g., see p. 324 of Varotsos and Lazaridou [38]). All the scales are in mV. Reprinted from Ref. [40], Copyright (2005), with permission from TerraPub.

We now proceed here to a description of what happened before the M_w6.6 EQ at 08:47 UT on May 13, 1995 (this EQ is labeled 'K'; see Fig. 4.5(b)).

The SES data and the prediction issued. On April 30, 1995, a three-page prediction was issued. The first page is reproduced in Fig. 7.9(a). It was a short paper under the title "Recent Seismic Electric Signal activities in Greece", the abstract of which stated: *"Three SES activities were recently recorded at IOA station. They might indicate that a pronounced series of EQs will occur in Greece with* M_s(ATH) $\approx$ 6.0 *units."* The two strongest SES activities (Fig. 1.11(a),(b)) were recorded on April 18 and April 19 (and were classified as such since they obey the criteria mentioned in Section 1.2). The second page reproduced in Fig. 7.9(b) contained the probable time-chart that will be followed as well as a map indicating the two candidate epicentral areas. The prediction text (Fig. 7.9(a)) stated that the *epicentral area located close to IOA was more probable*. The third page was a photocopy of the SES data, as collected through the real-time telemetric network; see Figs. 7.10 and 7.11 to which we now turn. (Recall that Fig. 1.11 depicts data collected with datalogger, see Section 1.1).

Figure 7.10 shows the intense SES activity recorded at IOA on April 18, 1995. It was mainly recorded on the NS short dipole array and on the 3 long dipoles. Figure 7.10(a) shows the recordings of the following 5 dipoles (see the map in Fig. 1.3): Two NS short dipoles ($L = 100$ and 184 m), one EW dipole ($L = 50$ m), and two long dipoles, labeled L and L$'$ (see Fig. 1.3(b)). Figure 7.10(b) depicts the recordings at the following 4 dipoles: one EW short dipole ($L \approx 50$ m), one short dipole ($L \approx 50$ m, labeled IOA, NS) which is almost parallel to the long dipoles that connect IOA with Perama village, and two long dipoles, labeled L-I and L$'$ in Fig. 1.3(b) (L$'$ coincides with that also depicted in Fig. 7.10(a)). The corresponding SES activity recorded on April 19, 1995, is given, as mentioned, in Fig. 7.11.

In addition, in Figs. 1.11(a) and 1.11(b), we have presented the SES recordings collected at two of the IOA sites, i.e., "B" and "C" (see the map in Fig. 1.3(c)), along with the variations of the two horizontal components of the magnetic field that have already been discussed in § 1.3.6.

Evaluation of the prediction. The prediction issued on April 30, 1995 shown in Fig. 7.9(a) discriminated between the two candidate epicenters, depicted in the prediction map of Fig. 7.9(b). One candidate epicenter was in western Greece (i.e., close to the Vartholomio-Killini area), while the second alternative was close to IOA. The prediction text clarified that the second solution seemed to be more compatible with the experimental facts. The predicted magnitude (for the latter solution) was (verbatim) *"*M_s(ATH) $\approx$ 5.5–*6.0 with an epicenter a few tens of km NW from IOA."* The actual epicenter (USGS [26]) was 40.14°N, 21.67°E, i.e., lying at a distance $\Delta r = 80$–90 km far from the predicted area. The fact that the actual magnitude M_s(ATH)$\approx$6.6 exceeded the predicted one M_s(ATH) $\approx$ 6.0 by $\Delta M = 0.6$, is consistent with what was naturally expected for larger epicentral distances than predicted "a few tens of km". As for the time-window, the EQ occurred on May 13, 1995, i.e., during the fourth week after the SES initiation, in accordance to the expected time chart; see § 1.3.1 case (b).

In summary, this prediction obeyed the tolerances (with respect to the time-window, epicenter and magnitude) for *successful* prediction. The latter is considered as such *if* $\Delta r \lesssim 100$ km, $\Delta M(=3\sigma) \leq 0.7$ and in addition Δt obeys the expected (time) limits (§ 1.3.1).

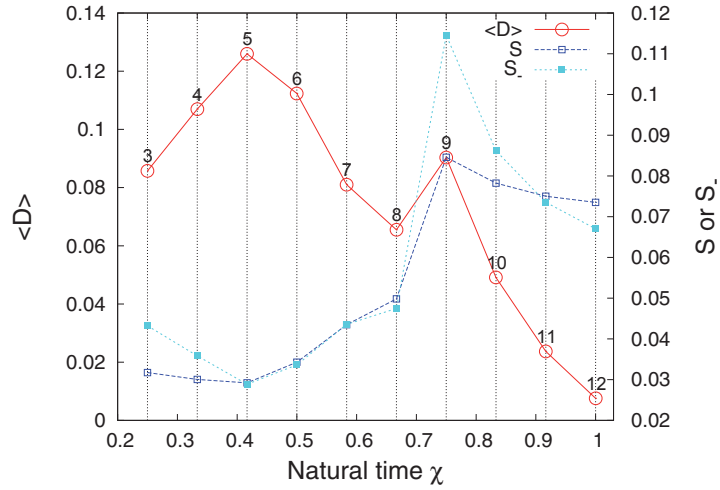

Fig. 7.12 Determination of the occurrence time of the major M_w6.6 EQ on May 13, 1995 (see also Fig. 7.13). The average distance $\langle D \rangle$ (red circles, left scale), the entropy S (open squares, right scale) and the entropy under time reversal S_- (filled squares, right scale) of the seismicity versus the natural time χ. The distance $\langle D \rangle$ drastically decreases only a few days before the occurrence of the mainshock, and the entropies S, S_-, become smaller than $S_u(=\ 0.0966)$ satisfying condition (7.4). The numbers correspond to the earthquakes listed in Table 6.1.

We now explain, following the *preliminary* procedure (§ 7.1.1), how the occurrence time of this EQ could have been identified in advance. We consider all EQs within the area A: $\mathrm{N}_{39.2}^{40.5}\,\mathrm{E}_{20.3}^{22.0}$ that occurred after the SES activity at IOA on April 18, 1995. These have already been listed in Table 6.1 and their analysis in natural time, explained in detail in § 6.2.1, resulted in the evolution of $\Pi(\phi)$, event by event, depicted in Fig. 6.3 (crosses). A careful inspection of this figure (in conjunction with that of Fig. 6.1) reveals that a coincidence is observed upon the occurrence of the EQ No. 12 on May 10, i.e., only 3 days before the mainshock. This is a *true* coincidence, because (see § 7.1.1): first, the average distance $\langle D \rangle$ between the curves of $\Pi(\phi)$ of the evolving seismicity and Eq. (7.1), as shown by the red circles in Fig. 7.12 is less than 10^{-2} at the coincidence; second, Fig. 7.13 – which is an excerpt of Fig. 6.3 depicting only the cases from Fig. 6.3(b) to Fig. 6.3(e) – shows that the evolving $\Pi(\phi)$, i.e., the red crosses, approach the blue curve, i.e., that of Eq. (7.1), from *below* upon the occurrence of the EQs No. 9, 10 and 11 (see Table 6.1) and the *coincidence* occurs at the event No. 12. Third, the criterion of Eq. (7.4) is obeyed, see Fig. 7.12. Finally, the occurrence time of the coincidence does not vary upon

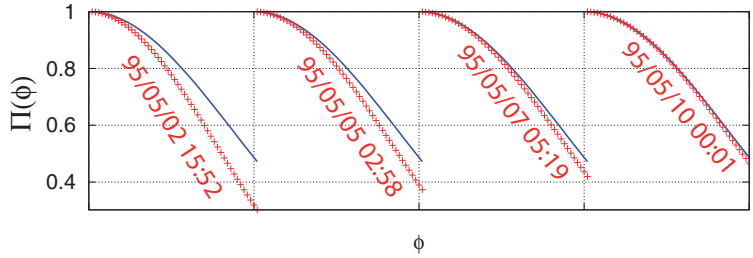

Fig. 7.13 Determination of the occurrence time of the major M_w6.6 EQ on May 13, 1995 (see also Fig. 7.12). The normalized power spectrum (red crosses) $\Pi(\phi)$ of the seismicity within the area $\mathrm{N}_{39.2}^{40.5}\,\mathrm{E}_{20.3}^{22.0}$ as it evolves event by event (whose date and time (UT) of occurrence are written in each panel) after the initiation of the SES activity on April 18, 1995. The excerpt presented here corresponds to Figs. 6.3(b) to 6.3(e). In each case only the normalized power spectrum in the window $0 < \phi < 0.5$ is depicted (separated by the vertical dotted lines), whereas the $\Pi(\phi)$ of Eq. (7.1) is depicted by the blue solid line.

changing *either* the magnitude threshold from $M_{thres} = 2.8$ to $M_{thres} = 2.9$ *or* the area from $\mathrm{N}_{39.2}^{40.5}\,\mathrm{E}_{20.3}^{22.0}$ to $\mathrm{N}_{39.5}^{40.4}\,\mathrm{E}_{20.5}^{22.0}$.

Thus, in short, applying the *preliminary* procedure, the occurrence time of this EQ could have been identified around 3 days in advance.

7.2.2 The major Eratini-Egion M_w6.5 earthquake on June 15, 1995

SES data and the prediction issued. This is the EQ labeled E in Fig. 4.5(b) and its prediction, as already explained in § 7.2.1, has been forwarded to the chairman (Sir James Lighthill) of the International Workshop held by the Royal Society (London, May 11–12, 1995).

Figure 4.5(a) shows the strong SES activity (labeled E) that was recorded on April 30, 1995, at the station VOL (Fig. 1.2). The operation of this station had started only six months before and hence the selectivity map, as well as the calibration of this station, was still unknown. No SES activity (simultaneous to that at VOL) was recorded at the other operating stations.

On the basis of the aforementioned SES activity, a two-page prediction was forwarded to the Government with some delay (caused by the occurrence of the aforementioned major EQ on May 13, 1995), i.e., on May 19, 1995. A photocopy is shown in Fig. 7.14, and its abstract clarifies that *a new strong EQ might hit Greece at a different epicentral area.* Despite the fact that the SES activity was recorded at a station not yet calibrated, the SES amplitude (10 mV/km) allowed the estimation, that the expected magnitude would be comparable to that of the EQ on May 13, 1995, i.e., around 6.6. Since the selectivity map of VOL was still unknown, the epicenter was estimated as follows: in addition to the short dipole arrays, the SES activity was recorded at two long dipoles (having almost the same direction, i.e., SSW and SW in respect to the Volos city, and lengths $L_1 = 5$ km and $L_2 \approx 22$ km)

THE UNIVERSITY OF ATHENS

DEPARTMENT OF PHYSICS
SOLID STATE PHYSICS SECTION
Knossou st. 36, Ano Glyfada
Athens 165 61, GREECE

P. Varotsos
Professor of Physics
Chairman of the Department of Physics

Athens, May 19, 1995

CONTINUATION OF THE SEISMIC ELECTRIC SIGNAL ACTIVITIES IN GREECE

by **P. Varotsos and M. Lazaridou**

Abstract: *The 6.6 earthquake of May 13, 1995 was preceded by seismic electrical activities recorded at IOA. A similar seismic electrical activity was subsequently recorded at* ***VOL.*** *It seems probable that a new strong earthquake (EQ) might hit Greece. This EQ should occur at a different epicentral area but with comparable magnitude. The present prediction is not equally reliable with the previous one, as VOL station is not yet calibrated (because it is operating during the last 6 months).*

On April 27 and 30, 1995 a prediction was issued based on seismic electrical signal (SES) activities recorded at IOA on April 18 and 19, 1995. This prediction was actually followed by a M_s=6.6 earthquake with a USGS epicenter at 40.0°N, 21.6°E (labelled with asterisk in Fig. 1). This area was previously considered to be *aseismic* because such EQ had not occurred there for a period more than 1000 years.

Since last September an experimental station is operating at VOL. The inspection of its records indicated that an SES activity was recorded on April 30 (i.e. **not** simultaneous with those earlier recorded at IOA) on both short and long dipole arrays. Although this station is not yet calibrated we might guess that it is precursor of an EQ similar to that of May 13, because its amplitude (10 mV/km) is comparable to those at IOA. The epicenter should be different due to the following facts:

(i) The two long dipoles installed at VOL (with lengths 22 km and 5 km) show comparable $\Delta V/L$-values thus indicating a non nearby source (and hence the neighbouring area of VOL should be excluded).

(ii) As the SES activity was not recorded at IOA, the areas belonging to IOA selectivity map (large hatched area in Fig. 1) should be excluded. As the epicenter of May 13 seems to belong to IOA selectivity map, the regions lying in its immediate vicinity (and especially those in its western side) should also be excluded.

(iii) As the SES activity was not recorded at ASS, the area belonging to ASS selectivity map (Fig. 1) i.e. that surrounded by the regions a, b, and c (and that of Chalkidiki peninsula and the neighbouring sea) should be excluded. (Note however that the VER area still remains as a candidate area as it is not well verified that it belongs to the ASS selectivity map. Unfortunately VER is out of operation).

(iv) As the SES activity was not recorded at KER, the area lying in the vicinity of Athens (and those in Peloponese) should be excluded. GOR is not operating and its immediate vicinity cannot be excluded.

(v) The central Aegean sea (recorded at ASS or at KER) should be excluded. However the area around Skiros and Alonisos islands cannot be excluded (they are of smaller probability).

By summarising: The new EQ might occur in the remaining part [i.e. after deleting the areas due to the points (i) to (v)] of continental Greece. The spectrum of the SES activity at VOL is **strikingly similar** to those recorded at IOA (on April 18, 19) thus indicating that the EQ of May 13 and the expected EQ might belong to the **same** tectonic process which, according to our opinion, is still going on. The time evolution might follow Fig. 22 of Varotsos et al (1993).

Fig. 7.14 The prediction issued on May 19, 1995, related to the M_w6.5 EQ that occurred on June 15, 1995 that was sent on May 20, 1995 at several institutes abroad.

with the same $\Delta V/L$ value; the latter fact indicated that the impending focal area should lie at a distance r appreciably larger than the dipole lengths, i.e. $r \gg L_1, L_2$ and hence $r/L_2 \gg 1$. As the ratio r/L_2 had to be, at least, around 4–5, the epicenter should lie at a distance more than ∼100 km from VOL. Furthermore as the SES activity was not recorded at the other four stations operating at that time, i.e. IOA, ASS, KER and PIR (see Fig. 1.2), we excluded as candidate epicenters the seismic areas belonging to their selectivity maps. We also excluded the area around the epicenter of the M_w6.6 earthquake which had just occurred on May 13, 1995, because the latter was preceded by SES activities at IOA.

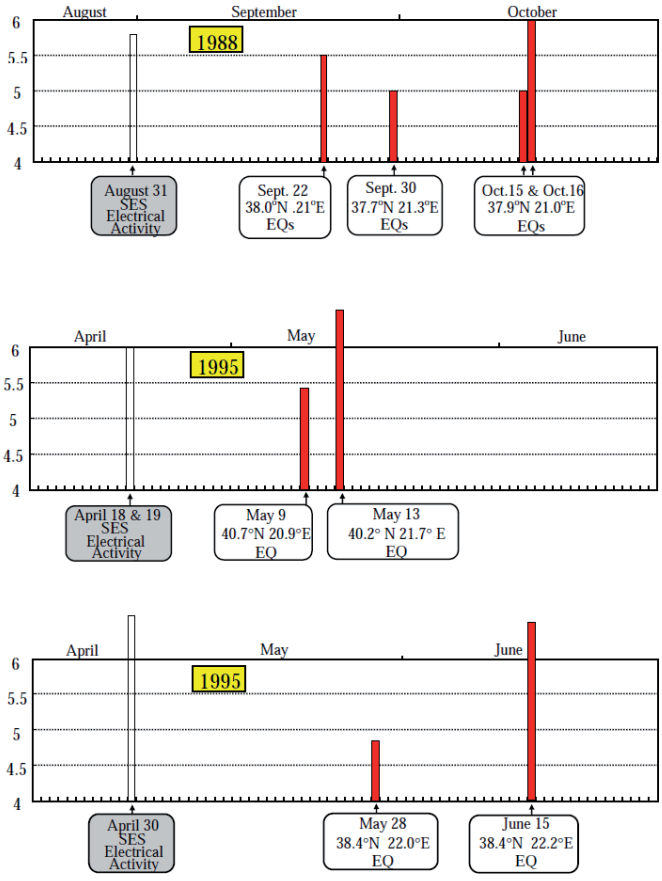

Fig. 7.15 Time evolution of the SES activities related with the 2 big EQs in Greece in 1995. For the sake of comparison, the case of Killini-Vartholomio destructive EQs in 1988 (i.e., fig. 28A of Varotsos and Lazaridou [38]) is also given. Open bars and full bars correspond to SES activities and EQs, respectively.

Thus, the prediction of the epicenter was summarized in the text of the prediction as follows: *"The new EQ might occur in the remaining part... of continental Greece"*. More precisely, the following areas were excluded from continental Greece: central western Greece, Chalkidiki area (including Thessaloniki), the area within a radius of at least ∼100 km around VOL, the Peloponnese, the neighboring area around Attica (i.e. Athens)

Table 7.2 All EQs within $N_{37.5}^{39.7}\,E_{21.5}^{25.0}$ that occurred after the initiation of the SES activity at VOL on April 30, 1995, until the M_w6.5 mainshock on June 15, 1995. Taken from Ref. [46].

No	Year	Month	Day	Hour	min	sec	Lat.	Lon.	Depth	M_L
1	1995	4	30	19	4	41	38.82	21.45	9	2.9
2	1995	5	2	8	26	56	38.20	21.76	32	2.7
3	1995	5	4	16	11	49	38.33	22.05	5	2.9
4	1995	5	6	1	44	12	37.70	21.46	10	2.5
5	1995	5	6	17	44	59	38.51	21.50	24	2.6
6	1995	5	6	23	10	21	38.44	21.80	5	2.6
7	1995	5	8	5	11	9	38.32	22.14	21	4.0
8	1995	5	9	12	48	34	38.32	22.09	10	2.5
9	1995	5	10	15	23	2	39.28	21.69	10	2.9
10	1995	5	12	7	25	13	39.12	24.48	31	3.6
11	1995	5	13	11	53	1	39.56	22.53	10	3.2
12	1995	5	13	13	31	55	38.52	22.04	5	3.3
13	1995	5	15	20	15	13	38.13	21.66	9	2.8
14	1995	5	16	5	15	44	38.97	23.18	33	3.6
15	1995	5	16	10	1	30	38.93	21.77	5	3.0
16	1995	5	17	23	5	25	39.73	21.89	5	2.9
17	1995	5	17	23	10	52	39.70	21.91	5	3.0
18	1995	5	17	23	20	30	39.74	21.97	5	3.1
19	1995	5	18	4	48	27	38.30	22.18	22	3.2
20	1995	5	19	23	19	49	38.24	21.87	11	2.7
21	1995	5	19	23	59	26	38.12	22.65	34	2.8
22	1995	5	20	20	32	33	38.41	21.79	9	2.9
23	1995	5	22	17	35	27	39.54	22.43	5	3.0
24	1995	5	23	2	56	49	39.51	22.25	10	2.7
25	1995	5	25	16	41	31	39.08	23.50	10	2.9
26	1995	5	25	20	32	11	39.74	21.57	35	3.0
27	1995	5	26	1	28	47	38.36	22.63	10	2.6
28	1995	5	26	7	9	25	38.36	22.00	5	2.9
29	1995	5	26	21	30	35	38.43	21.81	6	2.7
30	1995	5	28	16	14	44	38.90	25.04	49	3.2
31	1995	5	28	19	56	41	38.38	21.96	5	4.1
32	1995	5	28	20	9	14	38.40	21.90	5	3.0
33	1995	5	28	21	51	1	38.28	22.67	10	3.0
34	1995	5	29	13	3	3	37.61	22.78	5	2.8
35	1995	5	30	9	6	31	38.50	21.74	5	3.1
36	1995	5	31	12	25	42	39.21	22.88	10	3.0
37	1995	5	31	21	43	30	39.39	22.63	29	3.0
38	1995	6	1	14	4	53	38.13	21.74	5	3.2
39	1995	6	2	14	47	46	39.20	23.14	32	3.1
40	1995	6	4	18	47	35	38.50	22.25	5	2.6
41	1995	6	5	15	4	40	38.88	21.51	5	2.9
42	1995	6	5	16	50	24	38.86	21.47	5	2.9
43	1995	6	5	18	34	46	38.98	21.47	12	2.7
44	1995	6	5	18	35	31	38.97	21.47	7	2.7
45	1995	6	6	20	12	14	38.80	21.58	5	2.9
46	1995	6	12	20	27	7	38.21	22.22	39	2.9
47	1995	6	13	2	48	39	38.29	22.47	10	2.6
48	1995	6	14	11	8	41	38.04	21.54	28	2.5
EQ	**1995**	**6**	**15**	**0**	**15**	**51**	**38.37**	**22.15**	**26**	**5.6**

and, of course, the area of northern Greece around the major earthquake of May 13, 1995. Of the remaining small part of continental Greece, the area lying in the vicinity of GOR (this is a site shown in Fig. 1.1 lying in the vicinity of LAM; see Fig. 1.2) was the more probable. Recall that the region to the north of GOR, close to VOL, was already excluded in view of the same $\Delta V/L$ value collected at the long dipoles of VOL.

The actual epicenter of the mainshock at 00:15UT on June 15 was at 38.4°N, 22.3°E (USGS [26]) being consistent with the prediction, since it lies less than 40–50 km almost south of GOR. The actual EQ magnitude was $M_w = 6.5$, thus being also consistent with the predicted value 6.6.

As for the prediction of time, the last row of the prediction text indicated that the time evolution of seismicity might follow fig. 22 of Varotsos et al. [36]. What actually happened is shown in the lowest time-chart of Fig. 7.15 and the comparison to the predicted time chart (i.e., the upper one in Fig. 7.15), reveals a striking agreement. Note that a smaller EQ with $M_s(\text{ATH}) = 4.8$ occurred on May 28, 1995, at 38.4°N, 22.0°E, i.e. practically at the same area where the mainshock occurred almost two weeks later.

We now apply the *updated* procedure (§ 7.1.2) for the determination of the occurrence time of this EQ since the *preliminary* procedure can be found elsewhere [45, 46]. We consider all EQs (see Table 7.2) that occurred within the area A: $\text{N}_{37.5}^{39.7}\,\text{E}_{21.5}^{25.0}$ after the initiation of the SES activity recorded at VOL on April 30, 1995, and their M_0 values are estimated using the relation $\log_{10}(M_0) = 1.64M_L + \text{const.}$ as in § 7.2.1. The computation of κ_1 is extended, as mentioned in § 7.1.2, to all possible subareas of the area A and then the plot of the probability distribution $\text{Prob}(\kappa_1)$ versus κ_1 is constructed after the occurrence of each small event since April 30, 1995. Excerpts of these results that correspond to the period June 1 to June 12, 1995, are shown in Figs. 7.16(a) to 7.16(c) for three magnitude thresholds, i.e., $M_{thres} = 2.5$, 2.6 and 2.8. An inspection of these figures reveals that:

Upon the occurrence of the $M_L = 2.9$ event at 20:27 UT on June 12, 1995, the probability distribution $\text{Prob}(\kappa_1)$ maximizes at $\kappa_1 = 0.070$ for all three magnitude thresholds (see the arrows in Figs. 7.16(a) to 7.16(c)), thus signaling the impending mainshock that occurred almost two days later at 00:15 UT on June 15, 1995.

7.2.3 The major Aegean M_w6.5 earthquake on July 26, 2001

This is the major earthquake labeled A in Fig. 4.5. This figure also depicts the preceding SES activity which had duration of around two hours and was recorded at the station VOL on March 17, 2001. It was clearly detected at several short- and long-measuring dipoles located in a zone with spatial dimensions (a few tens km) × (several km), see Fig. 1.4. A copy from the recordings of the real-time telemetric network is given in Ref. [35] as well as in Ref. [41], while Fig. 7.17(a) depicts the digital recordings from the long-dipole

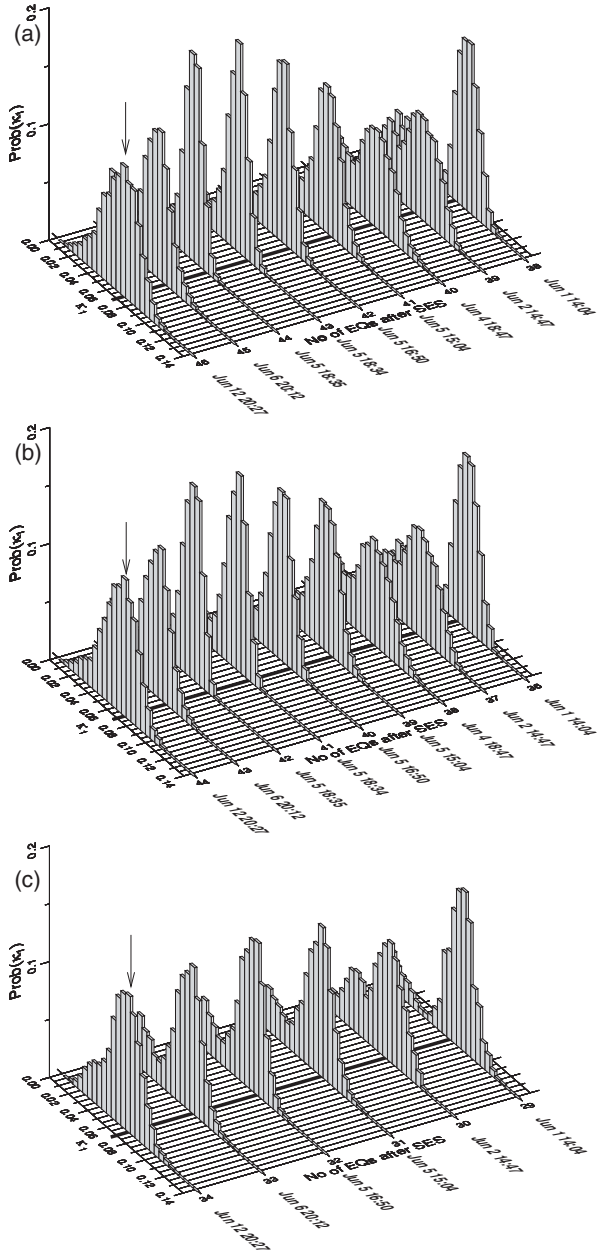

Fig. 7.16 Determination of the occurrence time of the M_w6.5 EQ on June 15, 1995. Prob(κ_1) versus κ_1 when considering the seismicity within the area $N_{37.5}^{39.7}$ $E_{21.5}^{25.0}$ since the initiation of the SES activity recorded at VOL on April 30, 1995. Excerpts for the period June 1 to June 12, 1995, are shown for (a) $M_{thres} = 2.5$, (b) $M_{thres} = 2.6$ and (c) $M_{thres} = 2.8$. The thick horizontal line corresponds to $\kappa_1 = 0.070$. The arrows show the maximum of Prob(κ_1) vs κ_1 observed at $\kappa_1 = 0.070$ on June 12, 1995, for all thresholds $M_{thres} = 2.5$, 2.6 and 2.8.

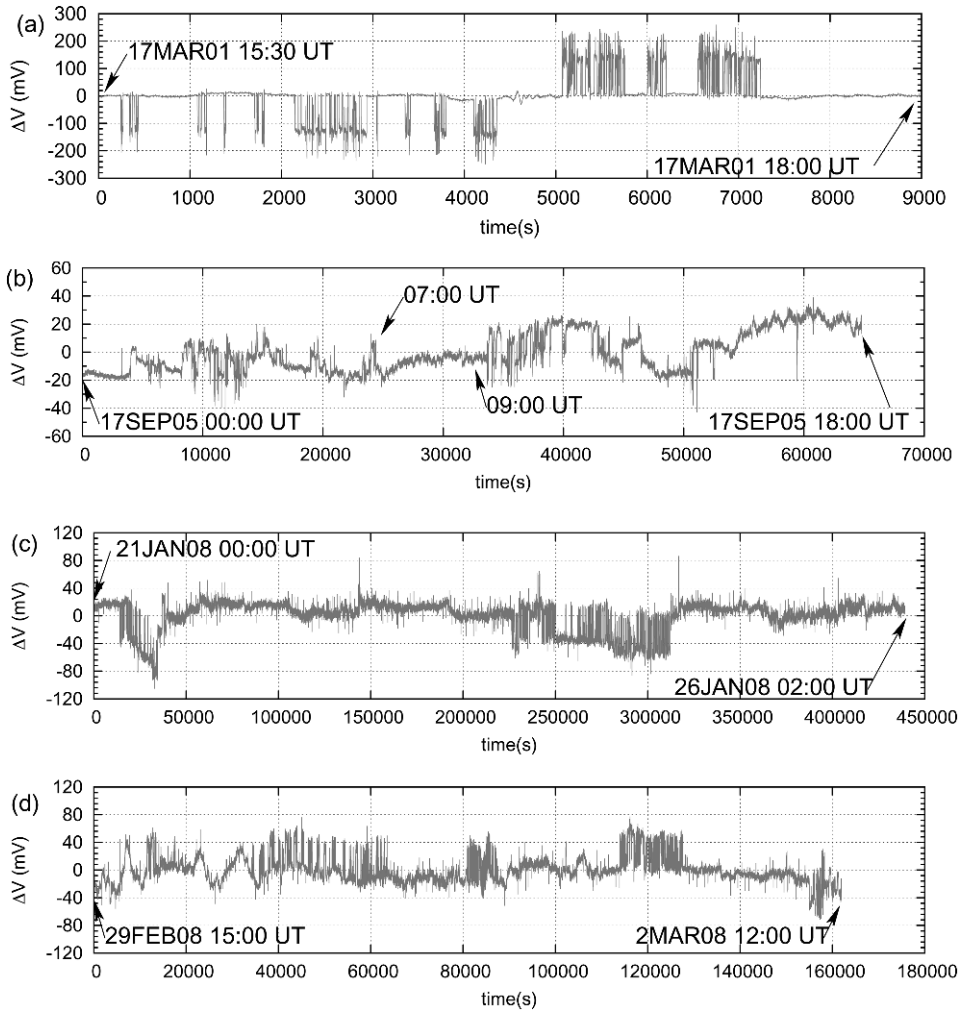

Fig. 7.17 SES activities before the major EQs with $M_w \geq 6.4$ since 2001. The short-duration SES activity (a) was recorded at VOL in 2001, while the three long-duration SES activities of (b), (c) and (d) at PIR in 2005 (b) and in 2008 (c, d) (see the text).

$V - S_{\Sigma B}$; see the map in Fig. 1.4. The digital recordings from all the measuring dipoles can be found in Ref. [41].

The epicenter of the impending seismic activity was estimated to be within the region marked with the broken line in Fig. 7.18. The procedure through which the SES activity was identified, as well as the expected epicenter and magnitude ($M \approx 6.5$) were determined, has been described in detail in Ref. [41] that was submitted for publication on March 25, 2001, i.e., almost four months before the EQ occurrence. Such a lead time seems to be in principle too long (note that a tentative explanation in terms of tectonics

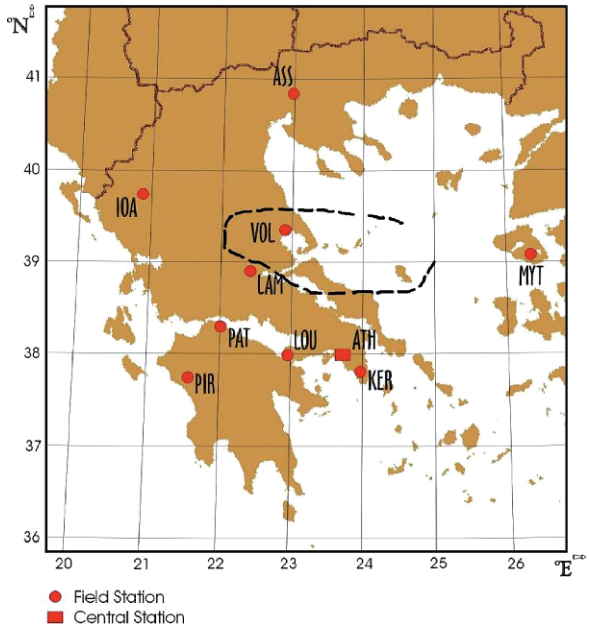

Fig. 7.18 The area 'bordered' by the broken curve (surrounding VOL) was the predicted area in Ref. [41] for the epicenter of the impending EQ related to the SES activity depicted in Fig. 7.17(a). Taken from Ref. [41].

and geodynamics of that seismic area has been discussed in Ref. [3]) but interestingly conforms with natural time analysis of the subsequent seismicity to which we now turn.

Since the *preliminary* procedure can be found elsewhere [45, 46], we present here the *updated* procedure (§ 7.1.2). We consider all EQs that occurred after the initiation of the SES activity at VOL on March 17, 2001, within the area A: $\mathrm{N}_{38.5}^{39.5}\,\mathrm{E}_{22.2}^{25.6}$, which includes the predicted area 'bordered' by the broken line in Fig. 7.18. The natural time analysis of seismicity (by using, as in § 7.2.1, the relation $\log_{10}(M_0) = 1.64 M_L + \text{const.}$, where M_L is taken from GI-NOA) was made, as explained in § 7.1.2, for all possible subareas of the area A and the resulting κ_1 values lead to the probability distribution $\text{Prob}(\kappa_1)$ of κ_1 shown in Fig. 7.19. An inspection of this figure shows that:

Upon the occurrence of the $M_L = 3.0$ EQ at 16:35 UT on July 25, 2001, which took place just eight hours before the mainshock (that occurred at 00:21 UT on July 26, 2001), $\text{Prob}(\kappa_1)$ vs κ_1 exhibits a maximum at $\kappa_1 = 0.070$ marked with arrows in Fig. 7.19(a), (b) and (c) for three magnitude thresholds, i.e., $M_{thres} = 2.8$, 2.9 and 3.0, respectively.

Concerning the actual magnitude of this mainshock, i.e, $M_w = 6.5$, it is comparable to the one estimated in advance [41].

As for its actual epicenter (see Table 7.1), it actually lies *within the predicted area* 'bordered' by the broken line in Fig. 7.18 and close to its eastern side.

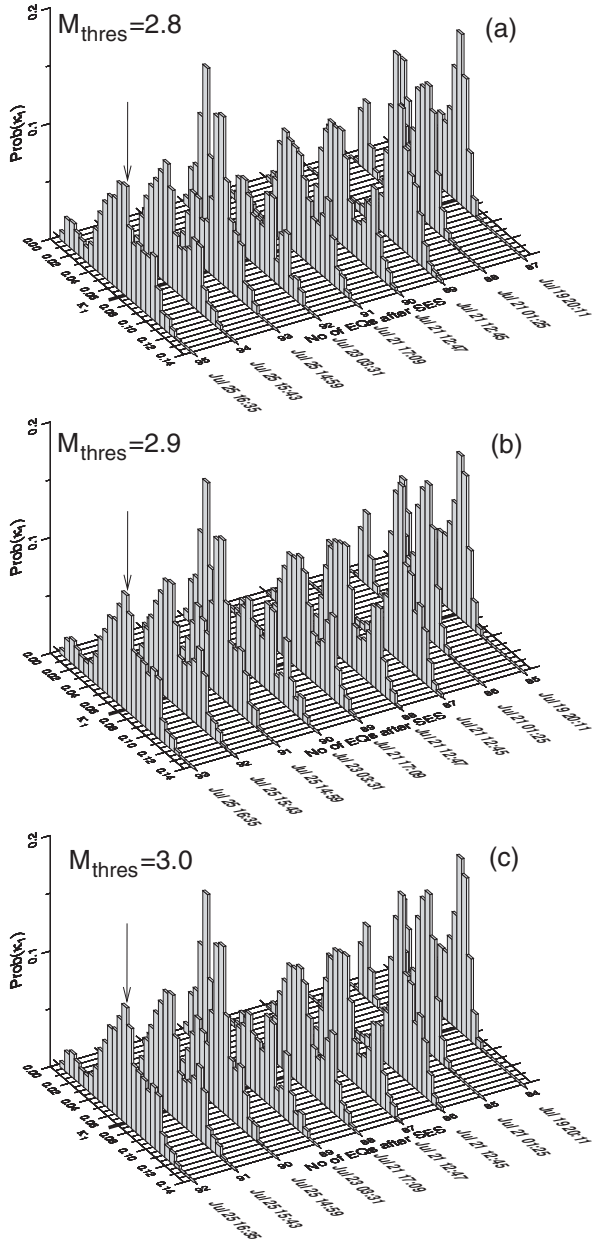

Fig. 7.19 Determination of the occurrence time of the major M_w6.5 EQ on July 26, 2001. Prob(κ_1) versus κ_1 when considering the seismicity within the area $N_{38.5}^{39.5}$ $E_{22.2}^{25.6}$ since the initiation of the SES activity recorded at VOL on March 17, 2001. The period July 19 to July 25, 2001, is shown for (a) $M_{thres} = 2.8$, (b) $M_{thres} = 2.9$, and (c) $M_{thres} = 3.0$. The thick horizontal line corresponds to $\kappa_1 = 0.070$. The arrows show the maximum of Prob(κ_1) vs κ_1 observed at $\kappa_1 = 0.070$ upon the occurrence of the $M_L = 3.0$ event at 16:35 UT on July 25, 2001.

Note that the predicted area is smaller than the one, i.e., $N_{38.5}^{39.5}\,E_{22.2}^{25.6}$, considered in the computation of κ_1 in the natural time analysis of seismicity. This could be understood in the following context. The (predicted) area in Fig. 7.18 is solely based on the SES characteristics governed by the electrical inhomogeneities in the Earth's crust, and hence does not necessarily coincide with the area considered in the updated procedure that involves the preceding small EQs that finally establish long-range temporal correlations. The same argument holds for the case of the EQ discussed in § 7.2.2.

7.2.4 The major M_w6.7 earthquake in southern Greece on January 8, 2006

Two intense SES activities, with a duration of several hours each, were recorded [42] at PIR station on September 17, 2005. They are shown together in Fig. 7.17(b), where we see that the first lasts until around 07:00 UT, while the second one starts after 09:00UT.

Almost one month later, a M_w5.7 EQ occurred in Western Greece on October 18, 2005, with an epicenter at 37.58°N 20.86°E (Table 7.1). USGS and Harvard reported that this EQ was mainly of thrust type, which, however, seemed to deviate from an earlier conclusion of Uyeda et al. [28] who had found that, for the EQs in the transform fault zone west of Kefallinia, the station PIR was mainly sensitive to strike–slip type EQs. In view of this deviation, doubts were raised whether any of the two SES activities of Fig. 7.17(b) were actually correlated with the EQ of October 18, 2005. As a result four days later, i.e., on October 22, 2005, a paper was submitted [42] raising the possibility that the two SES activities in Fig. 7.17(b) were in fact a one-day long-duration SES activity probably correlated with an impending strong EQ (*not* from the aforementioned area studied by Uyeda et al. [28]). Actually, at 11:34 UT on January 8, 2006, the M_w6.7 EQ occurred in southern Greece with an epicenter at 36.3°N 23.3°E, i.e., in an area different from the one studied earlier by Uyeda et al. [28].

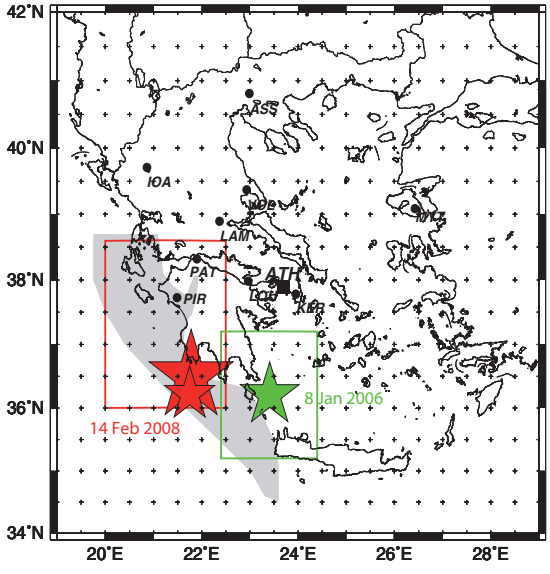

Fig. 7.20 A map showing the areas discussed in § 7.2.4, § 7.2.5 and § 7.2.6. The corresponding determination of the occurrence time for the M_w6.9 EQ on February 14, 2008 (red star), and the M_w6.7 EQ on January 8, 2006 (green star), was made by considering the seismicity within the red rectangle $N_{36.0}^{38.6}\,E_{20.0}^{22.5}$ and the green rectangle $N_{35.2}^{37.2}\,E_{22.4}^{24.4}$,respectively (see the text). The shaded area shows the PIR selectivity map updated in 2008 that was used later (§ 7.2.6) for the determination of the occurrence time of the major M_w6.4 EQ on June 8, 2008. Solid dots show the measuring stations of the telemetric network.

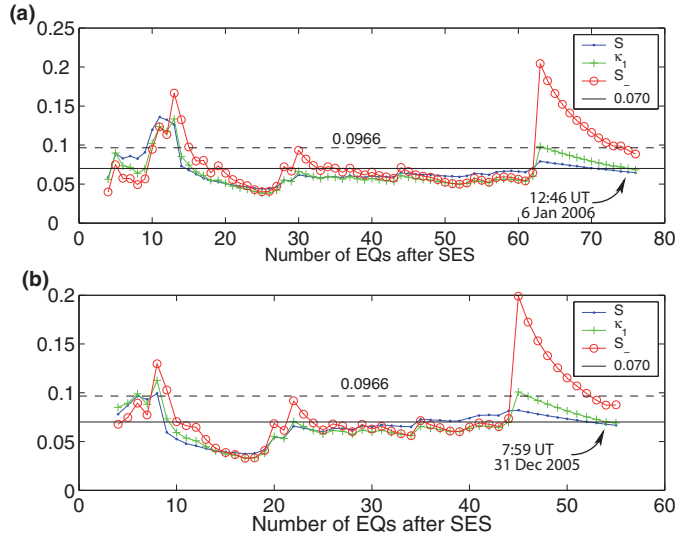

Fig. 7.21 Determination of the occurrence time of the major M_w6.7 EQ on January 8, 2006. The variance κ_1 (green), the entropy S (blue) and the entropy under time reversal S_- (red) of the seismicity within the green rectangular region of Fig. 7.20, as it evolves event by event after the long-duration SES activity recorded at PIR on September 17, 2005 (Fig. 7.17(b)): (a): For all small seismic events reported by GI-NOA, i.e., $M_{thres} = 2.6$ and (b): For seismic events with $M_{thres} = 3.0$. The horizontal solid line corresponds to $\kappa_1 = 0.070$ while the broken to $S_u = 0.0966$. Taken from Ref. [43].

We now follow the *preliminary* procedure explained in § 7.1.1. We set the natural time for seismicity zero at the initiation time of the SES activity recorded at PIR on September 17, 2005 (Fig. 7.17(b)) and form time series of seismic events in natural time for various time windows as the number of consecutive (small) EQs increases. We consider [42] all the small EQs (i.e., with $M_L \geq 2.6$) that occurred before the mainshock, within the region $\mathrm{N}_{35.2}^{37.2}\,\mathrm{E}_{22.4}^{24.4}$ surrounding the epicenter (see the green rectangular area in Fig. 7.20) according to the EQ catalog of GI-NOA (the corresponding M_0 values have been estimated from the relation $\log_{10}(M_0) = 1.64M_L + \text{const.}$ as in § 7.2.1). For each of the time windows, the following quantities have been computed: κ_1, $\langle D \rangle$, S and S_- and the results are plotted in Fig. 7.21(a). An inspection of this figure shows that κ_1 approaches the value 0.070 from *above* at 12:46 UT on January 6, 2005, i.e., almost two days before the occurrence of the mainshock. Furthermore, both S and S_- values at the coincidence are smaller than the value $S_u = 0.0966$ in accordance to Eq. (7.4). In addition, we confirmed that $\langle D \rangle$ is smaller than 10^{-2}. Finally, upon changing the magnitude threshold (i.e., taking $M_{thres} = 2.8$, instead of $M_{thres} = 2.6$) and studying a smaller region, i.e., $\mathrm{N}_{35.7}^{36.9}\,\mathrm{E}_{22.6}^{24.2}$, the occurrence time of the coincidence remains the same. Thus, we conclude that the conditions mentioned in § 7.1.1 for a *true* coincidence are obeyed. Despite this fact, and in order to shed more light on a point already tackled in § 7.1.1, we repeated the same calculation, but by imposing an even larger magnitude threshold, i.e., $M_{thres} = 3.0$. We then obtained the results depicted in Fig. 7.21(b) showing that the critical point is approached a week before the mainshock (note that *no* EQ with $M_L \geq 3.0$ occurred during that week). The difference in the results

is understood in the context already mentioned in § 7.1.1: if higher magnitude threshold is used, the description of the real situation approaching criticality becomes less accurate due to *'coarse graining'* [43] since the number of events is finite.

In summary, the natural time analysis of the seismicity subsequent to the long-duration SES activity at PIR enables the determination of the occurrence time of the M_w6.7 EQ on January 8, 2006, within a narrow range of around 2 days up to 1 week.

7.2.5 The two major M_w6.9 and M_w6.5 earthquakes in southwestern Greece on February 14, 2008

In this case, both short- and long-duration SES activities have been recorded (Table 7.1). The short one came first [44] and it was recorded (see Fig. 7.22(b)) on January 14, 2008, at the station PIR. Almost one week later, a long duration SES activity of the same polarity and amplitude was recorded also at PIR (Fig. 7.17(c)). The natural time analysis of the former (labeled PIR_3 in Table 4.6), which is of clear dichotomous nature, led [44] to the following parameters: $\kappa_1 = 0.070 \pm 0.005$, $S = 0.086 \pm 0.003$, $S_- = 0.070 \pm 0.005$, which obey the conditions in order to classify this signal as SES activity (note that it also satisfies the criteria mentioned in Section 1.2).

After this classification, the study of the seismicity in natural time was immediately started in the area A: $\mathrm{N}_{36.0}^{38.6}\,\mathrm{E}_{20.0}^{22.5}$ (determined by means of the procedure described in § 1.3.5) as publicized on February 1, 2008, by Varotsos et al. [44] (this area is marked with the red rectangle in Fig. 7.20). The corresponding M_0 values have been again estimated using the relation $\log_{10}(M_0) = 1.64 M_L + \text{const.}$ as in § 7.2.1. We now draw attention to the difficulty arisen if the *preliminary* procedure (§ 7.1.1) is applied to the present case. Within the area $\mathrm{N}_{36.0}^{38.6}\mathrm{E}_{20.0}^{22.5}$ studied since the initiation of this SES activity on January 14, 2008, two EQs with magnitudes $M_s(\mathrm{ATH}) \approx 5.5$ occurred on February 4, 2008, close to PAT associated with the SES activity at PAT on January 10, 2008; see Fig. 7.22(a). This results in the fact that the κ_1 value becomes very small, i.e., $\kappa_1 \approx 0$, at any small area surrounding the epicenters of these two EQs (see § 6.2.1; see also Ref. [54]). On the other hand, in the *updated* procedure (§ 7.1.2) the computation of κ_1 is extended to all possible subareas of the area $\mathrm{N}_{36.0}^{38.6}\mathrm{E}_{20.0}^{22.5}$. Then the plot of the probability distribution $\mathrm{Prob}(\kappa_1)$ versus κ_1 (shown in Fig. 7.23 for $M_{thres} = 3.2$) constructed after the occurrence of each small event exhibited a bimodal feature. The one mode, corresponding to nearly zero κ_1 values, results from the subareas that contain the aforementioned two EQs of magnitude 5.5. The other mode, maximized at $\kappa_1 = 0.070$, comes from subareas which do not include these two EQs. It is the latter mode that upon the occurrence of a small event at 04:07 UT on February 12, 2008; see the case marked with an arrow in Fig. 7.23, signifies the approach to the critical point. Two days later, i.e., at 10:09 UT on February 14, 2008, the M_w6.9 earthquake occurred at 36.5°N 21.8°E inside the area $\mathrm{N}_{36.0}^{38.6}\mathrm{E}_{20.0}^{22.5}$ specified in advance [44]. Two hours later, i.e., at 12:08 UT, a M_w6.5 EQ followed almost at the same epicenter.

At that period, beyond the *updated* procedure, the *preliminary* one was simultaneously applied. The latter procedure, upon avoiding the difficulty described above (i.e., by exclud-

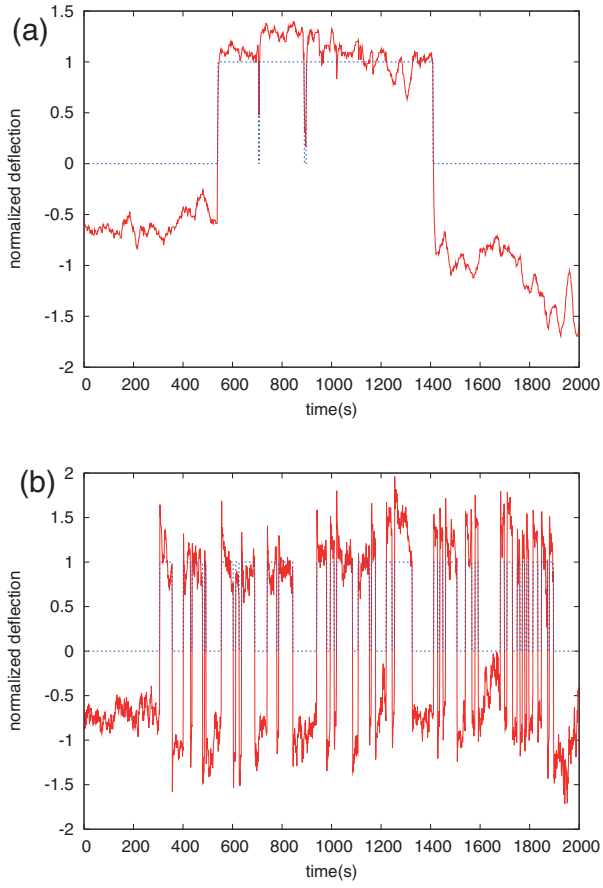

Fig. 7.22 The short duration SES activities recorded on January 10, 2008, at PAT (a) and on January 14, 2008, at PIR (b) in normalized units (i.e., by subtracting the mean value and dividing the results by the standard deviation) along with the dichotomous representation marked by the dotted (blue) line. Taken from Ref. [44].

ing the influence of the aftershocks around the two $M_s(\text{ATH}) \approx 5.5$ EQs that had already occurred close to Patras on February 4, 2008), had led to the conclusion that the critical point was approached somewhat earlier, i.e., on February 10, 2008 (note that the difference in the results of the two procedures can be understood on the basis of the discussion in § 7.1.1 concerning the *'coarse graining'* when using different magnitude thresholds). This explains why we were able to publicly announce on February 10, 2008, that the major EQ is imminent, as described in detail by Uyeda and Kamogawa [30, 31].

The M_w6.9 earthquake on February 14, 2008, according to USGS [26], is the strongest one in Greece since 1983. As explained above, all the parameters of this earthquake, i.e., the epicentral area (see the red rectangle in Fig. 7.20), the magnitude (recall that *only* when the expected M is larger than 6.0, a prediction is publicized) and the occurrence time were specified and announced in advance.

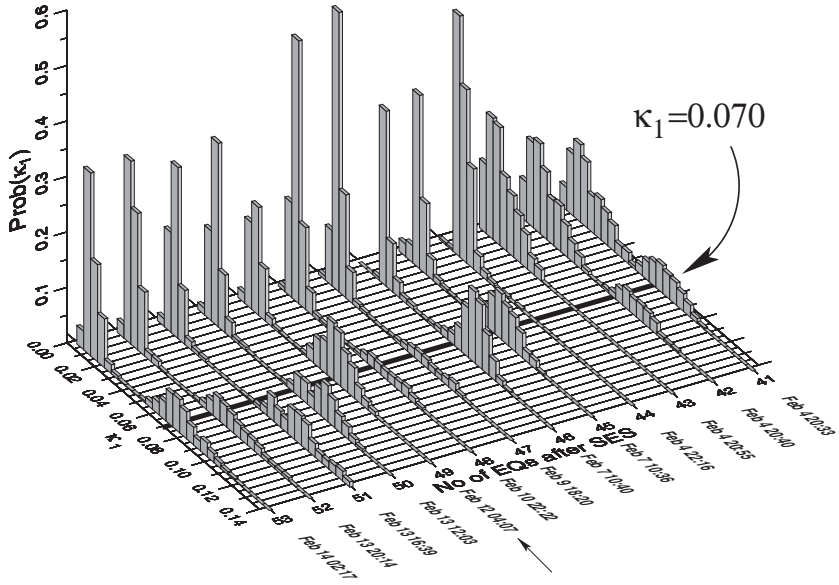

Fig. 7.23 Determination of the occurrence time of the major EQs on February 14, 2008. Study of the Prob(κ_1) versus κ_1 for the seismicity ($M_{thres} = 3.2$) that occurred within the area $N_{36.0}^{38.6}\,E_{20.0}^{22.5}$ after the short duration SES activity at PIR on January 14, 2008, depicted in Fig. 7.22(b). Taken from Ref. [21].

7.2.5.1 The experimental error in the epicentral location of small EQs and its influence on the determination of the occurrence time of an impending mainshock

The results depicted in Fig. 7.23 have been obtained upon adopting a reasonable experimental error in the determination of the epicentral coordinates of the small EQs involved in the aforementioned computation. In particular, two small EQs have been assumed to occur at different locations *iff* their reported epicentral coordinates differ more than $0.02^\circ \times 0.02^\circ$. In other words, the number of the possible subareas inside the estimated area A: $N_{36.0}^{38.6}\,E_{20.0}^{22.5}$ was counted after using a grid with "cells" having dimensions of $0.02^\circ \times 0.02^\circ$ and considering the reported epicentral coordinates of the small EQs. On the other hand, if we assume that the EQ epicentral coordinates, that have been reported with two decimals, are accurate and construct a grid based on these coordinates (adaptive grid), the population of the resulting possible subareas of the area $N_{36.0}^{38.6}\,E_{20.0}^{22.5}$ becomes markedly larger, thus leading to a somewhat different result. Namely, based on the latter assumption the computation was repeated and led to the results depicted in Figs. 7.24(a), 7.24(b) and 7.24(c) for $M_{thres} = 2.8$, 2.9 and 3.0, respectively. They show that a maximum of Prob(κ_1) versus κ_1 at $\kappa_1 \approx 0.070$ is simultaneously observed in all the three magnitude thresholds upon the occurrence of a $M_L = 3.4$ event at 10:40 UT on February 7, 2008, with epicenter at 38.37°N 20.32°E. This date, which is almost one week before the M_w6.9 mainshock of February 14, 2008, differs from the one (i.e., February 12, 2008) of the maximum observed in Fig. 7.23.

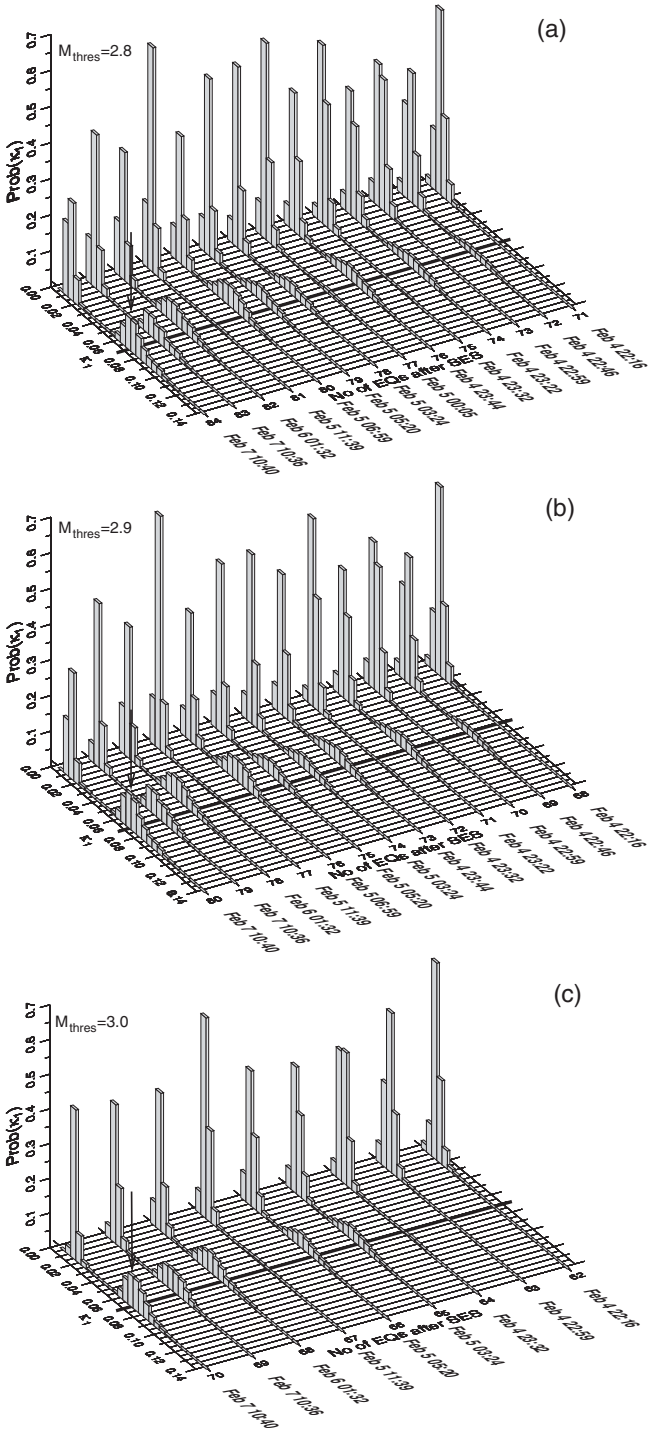

Fig. 7.24 Determination of the occurrence time of the major EQs on February 14, 2008, when considering the *assumption* discussed in § 7.2.5.1. Study of the Prob(κ_1) versus κ_1 for the seismicity for (a) $M_{thres} = 2.8$, (b) $M_{thres} = 2.9$, and (c) $M_{thres} = 3.0$ that occurred within the area $N_{36.0}^{38.6}$ $E_{20.0}^{22.5}$ after the SES activity at PIR on January 14, 2008, depicted in Fig. 7.22(b). The simultaneous maxima of Prob(κ_1) versus κ_1 at $\kappa_1 \approx 0.070$, marked with arrows, are observed upon the occurrence of a $M_L = 3.4$ EQ at 10:40 UT on February 7, 2008, with epicenter at 38.37°N 20.32°E.

In other words, we conclude that the date at which the maximum of Prob(κ_1) versus κ_1 at $\kappa_1 \approx 0.070$ is observed, depends somewhat on the accuracy considered in the epicentral coordinates of the small earthquakes involved in the computation.

This accuracy depends of course on several factors (including the density of the seismological network operating in the area investigated) and should be considered with care in each case separately. Since, however, the estimation of this accuracy is far outside of the scope of the present monograph, in all the other examples treated here, we assumed that the epicentral coordinates as reported are accurate.

We also note that a random experimental error (≈0.2 to 0.3) in the EQ magnitude, does not seem to affect the date of a *true* coincidence, as shown by Uyeda et al. [32] when applying the *preliminary* procedure.

7.2.6 M_w6.4 earthquake in the Peloponnese on June 8, 2008

This major EQ was preceded by that long-duration SES activity-lasted from February 29 to March 2, 2008 (see Fig. 7.17(d) which just reproduces the upper channel of Fig. 1.16). After subtracting the MT background with the procedure described in § 1.4.3.1, the signal was analyzed in natural time (see Section 4.11) and classified as an SES activity (note that it also obeys the criteria mentioned in Section 1.2).

The investigation of the subsequent seismicity was conducted at first (see Ref. [20]) in the area $\mathrm{N}_{37.0}^{38.6}$ $\mathrm{E}_{20.0}^{22.0}$, which is somewhat smaller than the PIR selectivity map known at that time. This was in an attempt to avoid as much as possible the influence of aftershocks of the M_w6.9 EQ at 36.5°N 21.8°E on February 14, 2008. This policy was considered justified, based on the notion that a criticality approach would take place in proper subareas simultaneously. At the same time, an attempt was also made to extend the area A to include the shaded area along the Hellenic Arc as shown in Fig. 7.20. This extension was based on the recent pieces of information for PIR selectivity map, including the occurrences of the aforementioned M_w6.9 EQ on February 14, 2008 (see § 7.2.5), associated with the SES activity of Fig. 7.17(c) and the M_w6.7 EQ at 36.3°N 23.2°E on January 8, 2006 (see § 7.2.4) following the SES activity of Fig. 7.17(b) at PIR [42]. In the study for the extended PIR selectivity map area (shaded region in Fig. 7.20), we raised the magnitude threshold to $M_{thres} = 3.9$, 4.0 and 4.1, because the extended area along the Hellenic Arc is highly seismic and there were too many (more than half a thousand) events to handle for $M_{thres} = 3.2$. This study showed that upon the occurrence of a M_s(ATH) = 5.1 EQ at 35.5°N 22.4°E at 23:26 UT on May 27 (practically May 28), 2008, the probability Prob(κ_1) exhibits a pronounced maximum at $\kappa_1 \approx 0.070$ marked by a vertical arrow in Fig. 7.25(a) drawn for $M_{thres} = 3.9$. Similar maxima at $\kappa_1 \approx 0.070$ appeared simultaneously for $M_{thres} = 4.0$ and $M_{thres} = 4.1$ (see Figs. 7.25(b) and 7.25(c), respectively), thus indicating that the critical point has been approached. This was reported on May 29, 2008, in Ref. [22]. Actually, at 12:25 UT on June 8, 2008, a M_w6.4 EQ occurred at 38.0°N 21.5°E, i.e., inside the candidate area $\mathrm{N}_{37.0}^{38.6}\mathrm{E}_{20.0}^{22.0}$ (see Ref. [20] publicized on March 20, 2008). It caused extensive damage (four people

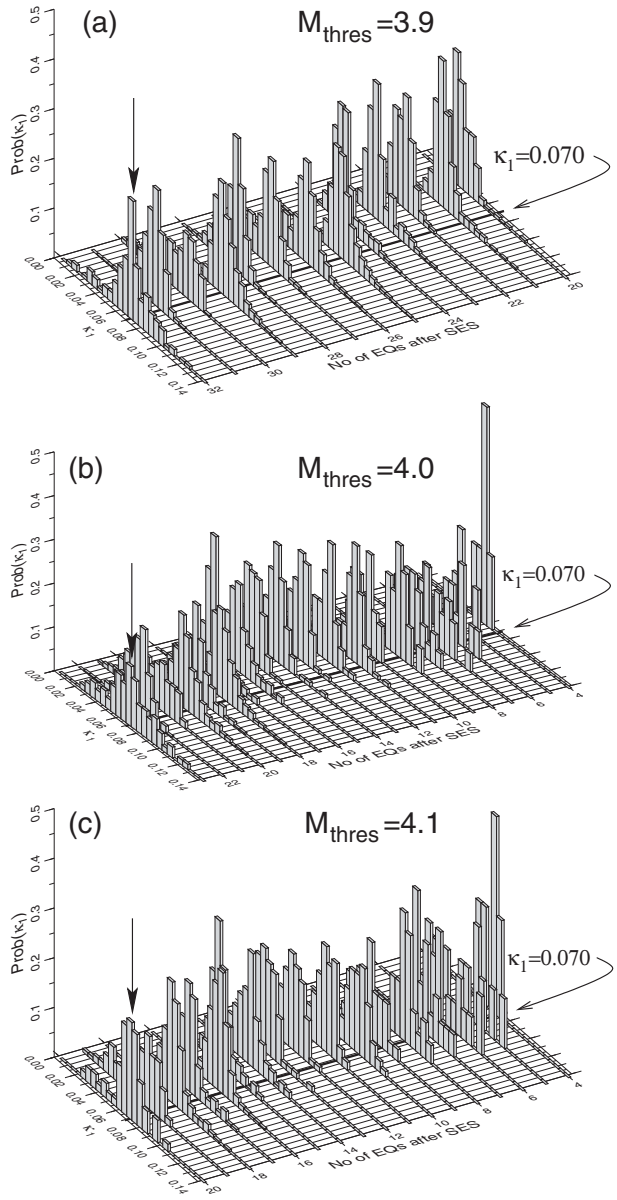

Fig. 7.25 Determination of the occurrence time of the major M_w6.4 EQ on June 8, 2008. Prob(κ_1) versus κ_1 of the seismicity $M_{thres} = 3.9$ (a), $M_{thres} = 4.0$ (b) and $M_{thres} = 4.1$ (c) within the shaded area shown in Fig. 7.20 subsequent to the long duration SES activity recorded at PIR during February 29 to March 2, 2008; see Fig. 7.17(d). The vertical arrows mark the maxima of Prob(κ_1) vs κ_1 at $\kappa_1 \approx 0.070$ that occurred at 23:26 UT on May 27, 2008 (practically May 28), and has been followed by the M_w6.4 on June 8, 2008. Taken from Ref. [22].

were killed while several hundred houses were seriously damaged). The magnitude 6–7 class EQ expected from the amplitude of the SES activity, as mentioned in the last paragraph of the Appendix of Ref. [21](which had been submitted for publication on March 21, 2008, i.e., after the completion of the analysis in natural time of the SES activity depicted in Fig. 7.17(d)), was reasonably well supported by the actual EQ magnitude [26], i.e., $M_w = 6.4$.

Thus, in short, all the parameters of the M_w6.4 earthquake that occurred at 12:25 UT on June 8, 2008, i.e., the epicentral area, the magnitude and the occurrence time, were specified and announced well in advance.

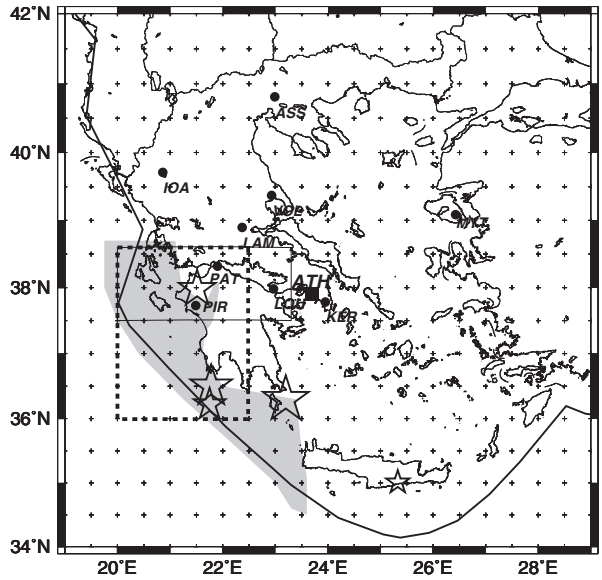

Fig. 7.26 The shaded area shows the up to that date (29 May 2008) addition to the PIR selectivity map. Solid dots show the measuring stations, while the stars denote the epicenters of the EQs discussed in Ref. [21] that were preceded by SES recorded at PIR. The rectangle with solid lines corresponds to the area $N^{38.6}_{37.5}E^{23.3}_{20.0}$ which is the preliminary selectivity map of PAT while the one with broken lines to $N^{38.6}_{36.0}E^{22.5}_{20.0}$, which is also shown (in red) in Fig. 7.20. Taken from Ref. [21].

7.3 Summary of all SES predictions issued along with all earthquakes of magnitude $M_w \geq 6.0$ in Greece since 2001

Table 7.1, as mentioned in § 7.2, compiles the information on what happened before *all* EQs with $M_s(\text{ATH}) \geq 6.0$ that occurred in Greece within the area $N^{41}_{36}\,E^{27}_{19}$ since 2001. We clarify that this Table also compiles *all* the predictions issued since 2001 considering that a prediction is issued *only* when the expected magnitude (on the basis of the SES amplitude) is $M_s(\text{ATH}) \geq 6.0$ (see § 7.2).

An inspection of Table 7.1 along with the contents of § 7.2.1 to § 7.2.6, which explain what happened before each of the major EQs with $M_w \geq 6.4$, leads to the following main conclusions:

(a) Concerning the natural time results of both the most significant SES activities and their subsequent seismicities until the corresponding mainshock since 2001: the results (see Table 7.1) reveal that in *all* cases but one (i.e., the one in 2003 in which the body wave magnitude mb = 5.6) with $M_w \geq 6.0$, natural time analysis enabled the classification of the relevant SES activity. This was documentated publicly well *before* the EQ occurrence.

(b) The cases mentioned in (a), include *all* five major EQs with $M_w \geq 6.4$ related to four mainshocks (Fig. 7.8). In each of these mainshocks, the occurrence time was identified within a narrow range, a few days to around one week or so, by analyzing in natural time the seismicity after the initiation of the SES activity. The same holds for the two major EQs during the previous decade (1990–2000, see Fig. 7.8) as shown by natural time analysis carried out in retrospect.

7.4 The volcanic-seismic swarm activity in 2000 in the Izu Island region, Japan

SES experimentation has been carried out by Uyeda and coworkers (e.g., Uyeda [27], Uyeda et al. [33, 29, 32], Orihara et al. [18]). The study has been made in two stages: In Stage 1 (1987–1995), only long dipole ($L = 1$–10 km) networks were used (Kinoshita et al. [9]; Takahashi et al. [24]; Nagao et al. [17]). In Stage 2, i.e., since 1996, short ($L \approx 100$ m) dipoles have been also installed. Several precursory changes similar to those observed in Greece have been recorded. They have been summarized by Uyeda et al. [33, 34] as well as in pp. 34–37 of Ref. [35].

Below we focus on the natural time analysis of the preseismic electrical anomalous changes and the seismicity observed in the 2000 swarm in Izu Island region, Japan.

This study by Uyeda et al. [32] is important because the nature of both seismic and electrical activities is vastly different from the Greek cases, i.e., the number of EQs subsequent to the initiation of the electrical disturbance was almost two orders of magnitude larger and the duration of electrical activity was around one order of magnitude longer than in Greek cases. Moreover, the swarm in the Izu Island region was considered closely related to volcanic/magmatic activity in contrast to the Greek cases.

In this Section we closely follow Uyeda et al. [32].

7.4.1 Natural time analysis of the precursory electric signals

The data collected. In the Izu Island region, a map of which is given in Fig. 7.27, electrical measurements were carried out in Niijima Island by means of 16 measuring electric dipoles (long and short ones) with sampling rate $f_{exp} = 0.1$ Hz. Anomalous electrical

changes were recorded [29] at two of these electric dipoles. Niijima Island is usually electrically almost noise free (Figs. 7.28(a) and 7.28(d)), the long (≈6 km) dipole "Wak-Air" connecting Wak (Wakago Village) and Air (Airport) and the short (≈30 m) dipole "Wak" in Wakago Village started to show innumerable visually clear unusual changes from 2 months before the onset of the swarm activity (i.e., on April 26, 2000) as illustrated in Figs. 7.28(b) and 7.28(c). Figure 7.29 shows the 3-year records of daily spectrum intensity at 0.01 ± 0.003 Hz after reducing noises common to "Air-Boe" dipole which showed no unusual changes by taking the intensity ratio of "Wak-Air" and "Air-Boe" dipoles. These two dipoles are almost in the same NS direction (see Fig. 7.27). They showed similar noises, mainly due to geomagnetic variations [29], while only "Wak-Air" dipole showed the unusual changes. In Fig. 7.29, it is clear that the anomalous changes were enhanced after the swarm activity started until the monitoring was interrupted in July and August 2000 by power failure caused by EQ shaking and typhoons.

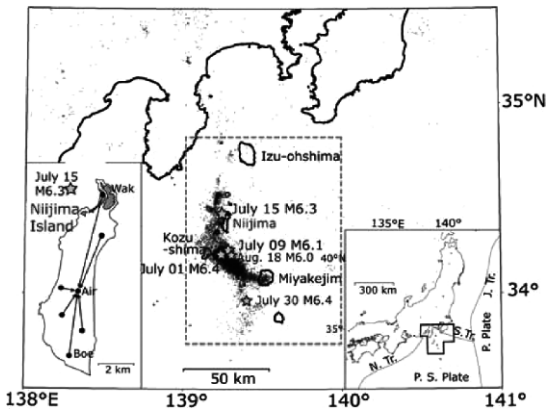

Fig. 7.27 Index map of the Izu Island region. Dots are $M_{JMA} \geq 0$ EQs from 1 June to September 30, 2000. Stars are $M_{JMA} \geq 6$ EQs. Right inset is a map of Japan with plate boundaries. P. plate, Pacific Plate; P. S. Plate, Philippine Sea Plate; N. Tr., Nankai Trough; S. Tr., Sagami Trough. Left inset shows the long dipole configuration of Niijima Island. A short dipole (not shown) is also installed at the far end of each long dipole centered at Air (Airport). Shaded parts near Wak are basaltic exposures. Broken rectangle shows the region of seismicity study $N^{34.8}_{33.7}E^{140}_{139}$. Taken from Ref. [32]. Copyright (2009), American Geophysical Union. Reproduced/modified by permission of American Geophysical Union.

These anomalous changes observed on almost perpendicularly oriented "Wak-Air" long and "Wak" short dipoles cannot be attributed to any source of "artificial" noise in this island of small population and no industry. Furthermore, the observed changes cannot be related with electrode noises, because the two dipoles were independent without a common electrode. As already mentioned in § 1.3.4, it is not uncommon that SES-sensitive sites are locally highly selective which means most sites are insensitive and a sensitive site is found only after a painstaking search through repeatedly moving temporary observation network, e.g. see Refs. [36, 10]. Moreover, as pointed out by Uyeda et al. [32], young basaltic rocks are exposed only at Wak area on the Island which otherwise exclusively consists of less conductive rhyolitic rocks (see the inset in Figure 7.27), suggesting highly heterogeneous underground electrical structure typical of a volcanic zone. According to volcanological studies [11, 25], Niijima Island was formed by rhyolitic activity in the Late Pleistocene and the basaltic exposure in Wakago area is less than a few thousand years old, the last basaltic magma phreatic activity being in the 9th century. It might be speculated [32] that the basaltic exposure is connected to the underground magma body, providing possible electrical channel for the transmission of electrical signals. In order to check these conjectures, which seem to be supported by a detailed geoelectrical modeling by Huang and Lin [6], a thorough electromagnetic exploration of the island is needed.

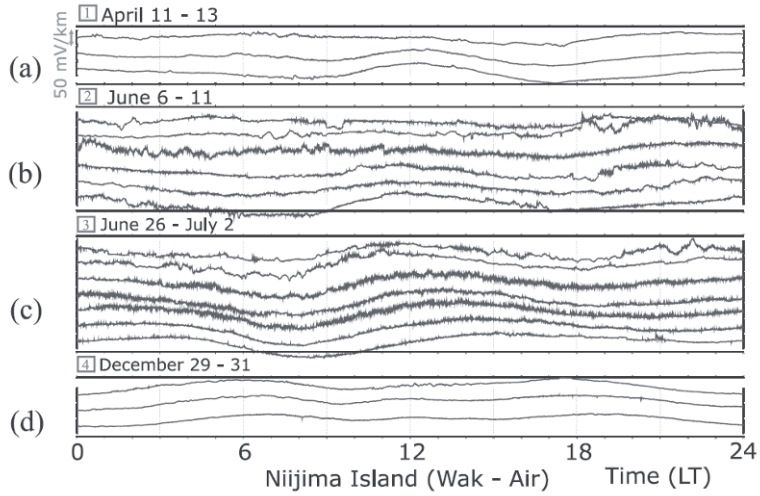

Fig. 7.28 Examples of typical 24-h records of the Wak-Air long dipole potential difference [29] (50 mV/km scale is indicated on the vertical axis). (a) Before 26 April. Records showed mainly smooth variations only. (b) During 2 months before the onset (26 June) of the seismic swarm activity. Numerous anomalous changes occurred. (c) Just after 26 June. Anomalous changes were more conspicuous. (d) After the cessation of the swarm activity, records resumed usual quietness. Time windows 1, 2, 3, and 4 are indicated in Fig. 7.29 (top). Taken from Ref. [32]. Copyright (2009), American Geophysical Union. Reproduced/modified by permission of American Geophysical Union.

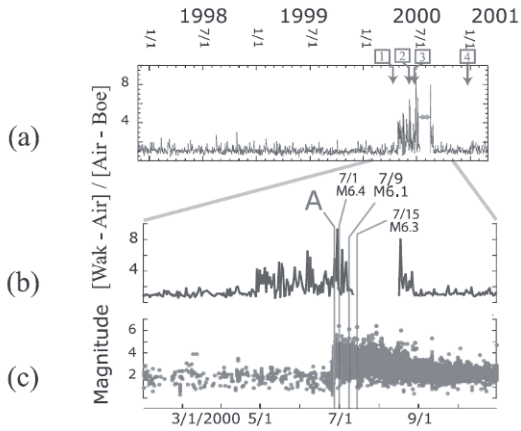

Fig. 7.29 Three-year record [29]. Time change of the 0.01 Hz spectral intensity ratio of geoelectric potential difference at Wak-Air and Air-Boe dipoles, Niijima Island. Anomalous changes started about two months before the seismic swarm (26 June to 29 August). The gap in data was caused by the system failure due to shaking and typhoons in July and August 2000. The numbers 1, 2, 3, and 4 correspond to those in Fig. 7.28. A is the date of the "true" coincidence. Taken from Ref. [32]. Copyright (2009), American Geophysical Union. Reproduced/modified by permission of American Geophysical Union.

Uyeda et al. [32] proceeded to the natural time analysis of the observed anomalous electric signals as follows. They first subtracted the MT background changes by applying a procedure similar to that explained in § 1.4.3.1 and the remaining signal was subsequently analyzed by applying natural time analysis as described earlier in Section 4.11. They found that these electrical disturbances had common characteristic properties with the SES activities in Greece. Thus, Uyeda et al. [32] concluded that they may well be called a SES activity.

7.4.2 Natural time analysis of Izu 2000 seismicity subsequent to the initiation of the SES activity

Uyeda et al. [32] applied the *preliminary* procedure explained in § 7.1.1. By setting natural time zero at the initiation time of the SES activity, analysis of the time series of seismic events in the rectangular region from N33.7° to N34.8° and from E139° to E140° as marked by broken lines (Fig. 7.27) was conducted using the JMA Catalog. In other words, the time series of seismic events in natural time was formed for increasingly longer time windows as the number N of consecutive EQs increased. Then, they computed $\Pi(\phi)$ for each of the time windows and examined its behavior. Specifically, the investigation was made for the period from 15:33 (LT) on April 30 (which was the occurrence time of the first EQ with magnitude greater than 3.5 after the initiation of the SES activity) until just before the occurrence of the first magnitude 6 class EQ very close to Niijima Island (July 1, 2000).

Uyeda et al. [32] used the magnitude in the JMA catalog (M_{JMA}) and employed Eqs. (6.10) to (6.13) to calculate the moment magnitude M_w. Then, the relation [5] $M_0 \propto 10^{1.5M_w}$ was used to obtain the values of the seismic moment M_0, as indicated in Fig. 2.1(b). The spatiotemporal evolution of the seismicity for magnitude threshold

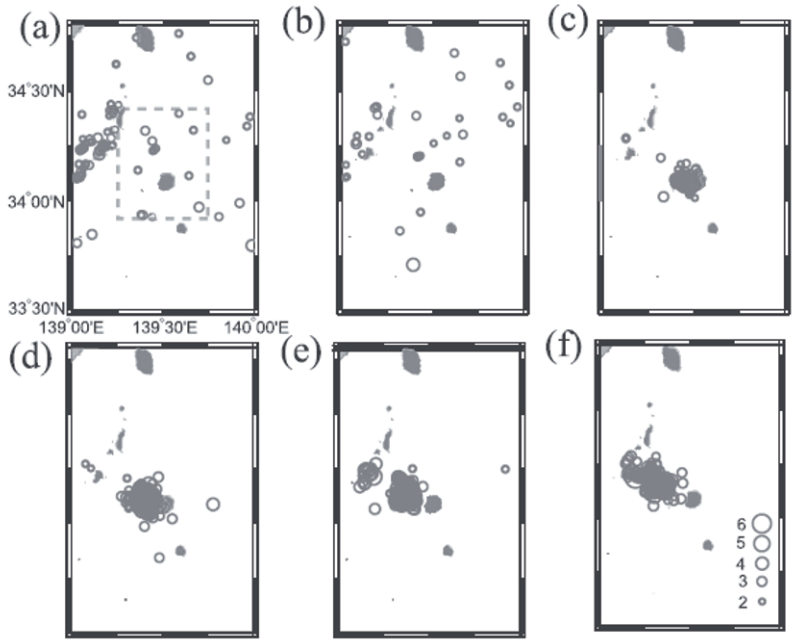

Fig. 7.30 Seismicity for $M_{JMA} \geq 2.0$ in the region $N_{33.7}^{34.8}E_{139}^{140}$ in the study period in 2000: (a) 1 January to 25 April, (b) 26 April to 25 June, (c) 26 June to 14:45 LT on 27 June, i.e., almost until the "true coincidence" (see Fig. 7.31), (d) after the "true coincidence" until 16:47 LT on 28 June, (e) 16:47 LT on 28 June until 15:31 LT on 29 June, and (f) after this, until the first magnitude 6 class EQ on July 1. Inset rectangle shows the smaller study area. Taken from Ref. [32]. Copyright (2009), American Geophysical Union. Reproduced/modified by permission of American Geophysical Union.

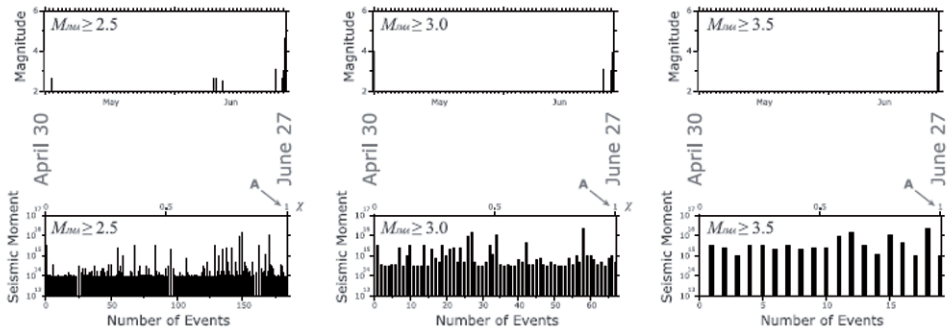

Fig. 7.31 The seismicity after 30 April until the "true coincidence" on 27 June for magnitude thresholds (a) $M_{JMA} \geq 2.5$, (b) $M_{JMA} \geq 3.0$, and (c) $M_{JMA} \geq 3.5$ for (top) conventional time and (bottom) natural time. In the bottom panel, the number of events (instead of χ) is given in the horizontal axis for the reader's convenience. Taken from Ref. [32]. Copyright (2009), American Geophysical Union. Reproduced/modified by permission of American Geophysical Union.

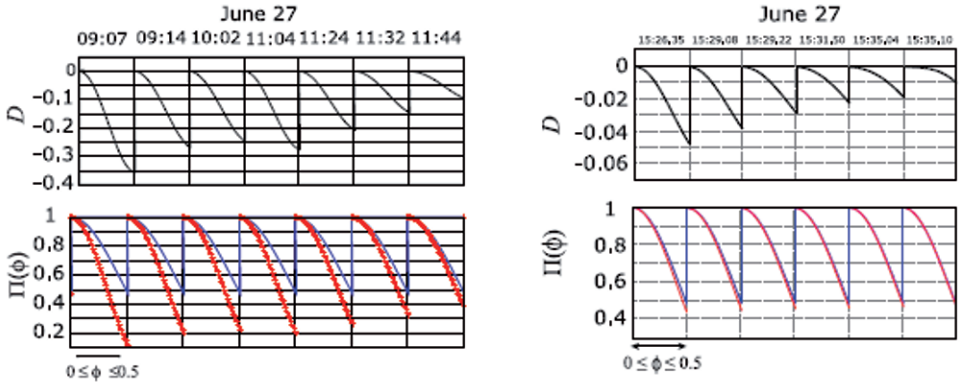

Fig. 7.32 (bottom) Time evolution of $\Pi(\phi)$ for $0 \leq \phi \leq 0.5$ of the seismic activity for $M_{JMA} \geq 3.0$ when the calculation was started on 30 April. $\Pi(\phi)$ curves (red) fall on the theoretical $\Pi(\phi)$ curves (blue) calculated from Eq. (7.1) as critical stage is approached. (top) The difference D between the two curves. (a) Examples for the morning hours of 27 June. (b) At the last six events which occurred at 15:26:35, 15:29:08, 15:29:22, 15:31:50, 15:35:04, and 15:35:10 LT on 27 June until the "true coincidence". Taken from Ref. [32]. Copyright (2009), American Geophysical Union. Reproduced/modified by permission of American Geophysical Union.

$M_{JMA} \geq 2.0$ in the studied region is shown in Figs. 7.30(a) to 7.30(f). The readings of the seismicity in natural and conventional time frames until the coincidence marked A on June 27 are shown in Fig. 7.31 for three different magnitude thresholds. Figures 7.30(a) to 7.30(f) show how nonlinearly the two time frames are interconnected. One may notice that the natural time covered in Figs. 7.30(a) to 7.30(f) is practically from June 26 to June 27, indicating that important changes took place in a short period even before the bulk of the swarm activity (see Fig. 7.29). Figure 7.32 (bottom) clearly shows that for magnitude threshold 3.0 as an example, the computed $\Pi(\phi)$ curve approaches the critical $\Pi(\phi)$ curve from *below* on June 27, 2000, a few days before the first $M \geq 6$ earthquake of July 1,

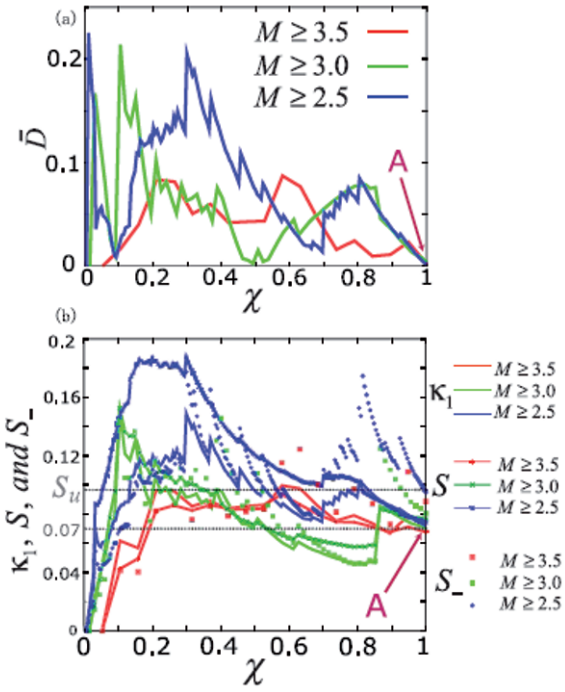

Fig. 7.33 $\overline{D} \equiv \langle D \rangle$, κ_1, S, and S_- of the evolving seismic activity versus the natural time χ. The calculation was started on 30 April and continued until the true coincidence A on 27 June just 4 days before the first M $\geq$ 6 class EQ on 1 July. Three magnitude thresholds ($M_{JMA} \geq 2.5$), ($M_{JMA} \geq 3.0$), and ($M_{JMA} \geq 3.5$) are considered. (a) $\overline{D}$ is plotted and (b) the quantities κ_1, S, and S_- are shown with the symbols depicted. Taken from Ref. [32]. Copyright (2009), American Geophysical Union. Reproduced/modified by permission of American Geophysical Union.

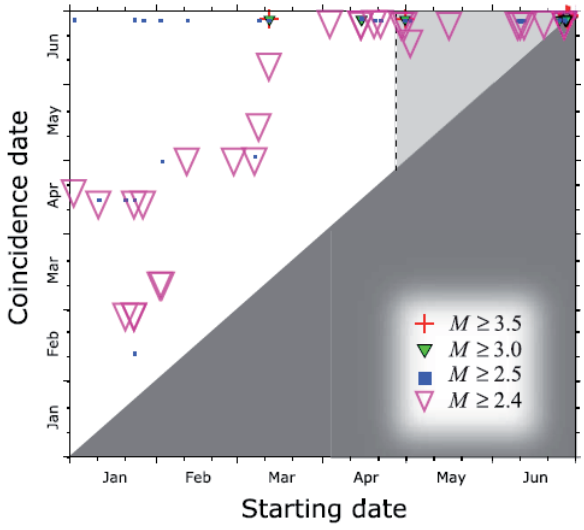

Fig. 7.34 Coincidence date versus the starting date of calculation for four magnitude thresholds. The SES activity started on April 26. The shaded triangular area is irrelevant because the coincidence has to be only in the unshaded area. Taken from Ref. [32]. Copyright (2009), American Geophysical Union. Reproduced/modified by permission of American Geophysical Union.

2000. The approach of the two curves is more clearly demonstrated in the upper panel of Fig. 7.32, in which D is plotted.

Moreover, Fig. 7.33 depicts $\langle D \rangle$, κ_1, S, and S_-, as they evolved event by event during the whole period (April 30 to June 27). This figure also shows that all three different magnitude thresholds resulted in approximately the same time of coincidence on June 27, supporting the self-similar structure of the process concerned [32].

As to the spatial self-similar nature of the process, a similar calculation was made for a smaller region depicted in Fig. 7.30(a). The results showed the same behavior. Thus, the coincidence on June 27 is considered as *true* coincidence since all the conditions mentioned in § 7.1.1 are obeyed. It may be added here that in fact, Uyeda et al. [32] made the calculations until the last event before the first M $\geq$ 6 class EQ of July 1 and there was another case with $\kappa_1 = 0.070$. But this second case was discarded because it did not satisfy the entropy criterion for true coincidence, i.e., the condition (7.4).

Figure 7.34 shows the coincidence dates (vertical axis) when the calculations were started on the dates shown on the horizontal axis for four magnitude thresholds. The calculation with M2.4 threshold was added here in order to check if the *true* coincidence A recognized by the abovementioned three threshold calculations satisfies the magnitude threshold invariance even for M2.4 threshold. Figure 7.34 clearly shows that *true* coincidence is reached at a time close to the date of the first M $\geq$ 6 shock, i.e., late June, only when the calculation was started around the initiation date of the SES activity, which is indicated by a vertical broken line in Fig. 7.34. It was found that the self-similarity condition for M2.4 threshold was useful for identifying *true* coincidence. One may wonder if the uncertainty in magnitude (or moment) determination bothers this kind of analysis.

Hence, Uyeda et al. [32] have conducted simulation test giving 0.2–0.3 random error of magnitude and concluded that the date of the *true* coincidence is not affected.

7.4.3 Main conclusions from the study of the Izu 2000 case

Uyeda et al. [32], after analyzing in natural time both the SES activity started on April 26, 2000, as well as the subsequent seismicity, as explained in § 7.4.1 and § 7.4.2 respectively, obtained the following main conclusions:

First, before the first magnitude 6 class EQ on July 1, one *true* coincidence was observed on June 27. Thus, the analysis in the natural time domain of the seismicity led to an estimation on the date of the impending large EQ of July 1, 2000, with a narrow time window of the order of a few days.

Second, it has been demonstrated that starting the calculation more than 2 weeks earlier than the initiation time of the SES activity does *not* result in *true* coincidence, whereas starting the calculation at later time does so. This is consistent with Greek cases in which natural time zero was set at the time of SES activity initiation.

7.5 Results from California: the $M_S 7.1$ Loma Prieta earthquake on October 18, 1989

This is the best-known case in the USA for which clear precursory electromagnetic variations have been reported. Almost one month before this earthquake, i.e., on September 12, 1989, magnetic field variations were recorded at a site just 7 km from the earthquake epicenter [4, 1] similar to those accompanying the SES activities in Greece for earthquakes with M6.5 or larger [56] (see § 1.3.6).

Table 7.3 The seismic data (reported from the Northern California Earthquake Data Center, http://www.ncedc.org/ncedc/catalog-search.html, as they appeared on January 8, 2010) analyzed in natural time. The magnitude M corresponds either to M_L or M_D. It is converted to seismic moment according to $M_w = \text{M}$. Taken from Ref. [53].

Number	Magnitude M	Date	Time(UT)	Latitude	Longitude
1	2.7	1989/9/16	18:41:24	37.33	−121.70
2	3.2	1989/9/28	15:42:37	36.57	−121.11
3	2.7	1989/10/1	12:21:37	38.15	−121.90
4	3.0	1989/10/1	13:10:24	38.14	−121.93
5	3.2	1989/10/1	13:19:27	38.16	−121.93
6	3.1	1989/10/1	22:08:35	36.56	−121.15
7	3.1	1989/10/1	22:09:17	36.56	−121.15
8	2.7	1989/10/2	11:20:19	38.15	−121.91
9	2.6	1989/10/6	15:53:36	37.32	−122.11
10	3.3	1989/10/8	12:36:46	36.44	−121.01
11	2.7	1989/10/9	11:51:24	37.63	−121.70
12	2.7	1989/10/9	12:06:02	37.29	−122.09
13	3.1	1989/10/9	12:42:03	37.63	−121.69
14	2.8	1989/10/13	12:22:11	36.63	−121.08
15	7.0	1989/10/18	00:04:15	37.04	−121.88

Following Ref. [53], in order to determine the occurrence time of the impending mainshock, we analyze in natural time all the earthquakes (see Table 7.3) that occurred after September 12, 1989, which is the date of the initiation of the aforementioned (SES like) precursory magnetic field change, within the area A: $\text{N}_{36.2}^{38.5}\text{W}_{122.7}^{120.7}$ surrounding the Loma Prieta earthquake epicenter. The seismic data used here are from the Northern California Earthquake Data Center and the relevant epicenters are depicted in Fig. 7.35. We set the natural time zero at the initiation time of the magnetic field change, and then formed time

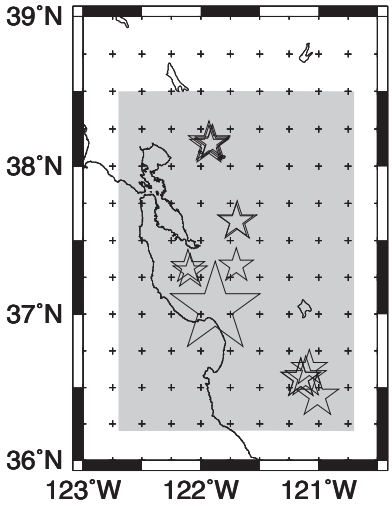

Fig. 7.35 The area $N_{36.2}^{38.5}W_{122.7}^{120.7}$ (shaded) surrounding the epicenter of the Loma Prieta earthquake (largest star) in which the seismicity after the initiation on September 12, 1989, of the precursory magnetic field variations [4, 1] is analyzed in natural time. Taken from Ref. [53].

series for the area A each time a small earthquake (with magnitude M exceeding a certain threshold M_{thres}, i.e., $M \geq M_{thres}$) occurred. The quantity κ_1 for each of the time series was computed for the pairs (χ_k, Q_k). The quantity Q_k was taken as the seismic moment M_{0k} of the k-th event (see Fig. 2.1(b)), calculated from the relation $\log_{10} M_0 \approx 1.5 M_L + \text{const.}$ (H. Kanamori, personal communication).

Applying the *updated* procedure (§ 7.1.2), in order to check whether criticality has been approached at the occurrence of a new event k within the area A, we construct all the possible subareas of $A_{M_{thres}}$ that necessarily include the event k and examine whether their κ_1 values reveal a probability distribution Prob(κ_1) maximized at 0.070. We considered only earthquakes with $M > 2.5$ in order to have homogeneous and complete catalog (see Ref. [2]). In other words, we take $M_{thres} = 2.6$. The results are depicted in Fig. 7.36(a), which shows how Prob(κ_1) versus κ_1 evolves upon the occurrence of each event before the October 18, 1989, M_s7.1 Loma Prieta earthquake. We see that Prob(κ_1) maximizes at $\kappa_1 = 0.070$ upon the occurrence of a 2.8 event at 12:22 UT on October 13, 1989, i.e., almost 5 days before the main shock. Upon repeating the calculation for larger magnitude thresholds, i.e., $M_{thres} = 2.7$ and 2.8, see Figs. 7.36(b) and 7.36(c), respectively, we find again that the maximum of Prob(κ_1) versus κ_1 is observed at $\kappa_1 = 0.070$ on October 13, 1989.

In summary, we analyzed in natural time the small earthquakes that occurred after the initiation on September 12, 1989, of the (SES-like) magnetic field variations in the area surrounding the epicenter of the M_s7.1 Loma Prieta earthquake. We find that Prob(κ_1) versus κ_1 exhibits a maximum at $\kappa_1 = 0.070$, for $M_{thres} = 2.6$, 2.7 and 2.8, on October 13, 1989, i.e., *five days before* the occurrence of the mainshock.

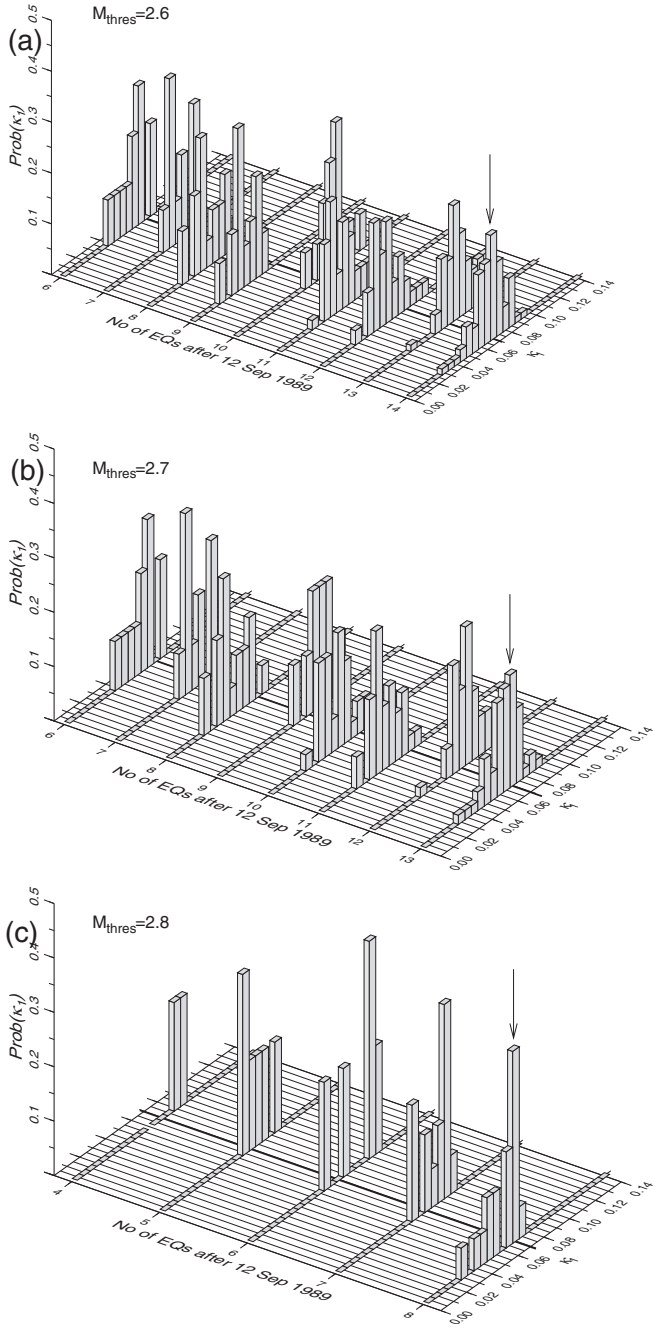

Fig. 7.36 Detemination of the occurrence time of the M_s7.1 Loma Prieta EQ on October 18, 1989. Prob(κ_1) versus κ_1 for the seismicity in the area $\mathrm{N}_{36.2}^{38.5}\mathrm{W}_{122.7}^{120.7}$, for $M_{thres} = 2.6$ (a), $M_{thres} = 2.7$ (b) and $M_{thres} = 2.8$ (c) subsequent to the initiation on September 12, 1989, of the precursory (SES like) magnetic field variations reported in Refs. [4, 1]. The last event corresponds to the magnitude 2.8 earthquake that occurred at 12:22 UT on October 13, 1989 with an epicenter at 36.63°N 121.08°W (see Table 7.3). Taken from Ref. [53].

References

1. Bernardi, A., Fraser-Smith, A.C., McGill, P.R., Villard, O.G.: ULF magnetic field measurements near the epicenter of the Ms 7.1 Loma Prieta earthquake. Physics of The Earth and Planetary Interiors **68**, 45–63 (1991)
2. Davidsen, J., Grassberger, P., Paczuski, M.: Networks of recurrent events, a theory of records, and an application to finding causal signatures in seismicity. Phys. Rev. E **77**, 066104 (2008)
3. Dologlou, E., Hadjicontis, V., Mavromatou, C.: Electrical precursors of earthquakes in Aegean sea during the last decade (1997-2007). Natural Hazards and Earth System Science **8**, 123–128 (2008)
4. Fraser-Smith, A.C., Bernardi, A., McGill, P.R., Ladd, M.E., Helliwell, R.A., Villard, O.G.: Low-frequency magnetic-field measurements near the epicenter of the Ms-7.1 Loma Prieta earthquake. Geophys. Res. Lett. **17**, 1465–1468 (1990)
5. Hanks, T.C., Kanamori, H.: Moment magnitude scale. J. Geophys. Res. **84(B5)**, 2348 (1979)
6. Huang, Q., Lin, Y.: Selectivity of Seismic Electric Signal (SES) of the 2000 Izu earthquake swarm:a 3D FEM numerical simulation model. Proc. Jpn. Acad., Ser. B **86**, 257–264 (2010)
7. Jaume, S.C., Sykes, L.R.: Evolving towards a critical point: A review of accelerating seismic moment/energy release prior to large and great earthquakes. Pure Appl. Geophys. **155**, 279 (1999)
8. Kerr, R.A.: Quake prediction tool gains ground. Science **270**, 911–912 (1995)
9. Kinoshita, M., Uyeshima, M., Uyeda, S.: Earthquake prediction research by means of telluric potential monitoring, Progress Rep. 1. Bull. Earthq. Res. Inst. **64**, 255–311 (1989)
10. Kondo, S., Uyeda, S., Nagao, T.: The selectivity of the Ioannina VAN station. J. Geodynamics **33**, 433–461 (2002)
11. Koyaguchi, T.: Evidence for two-stage mixing in magmatic inclusions and rhyolitic lava domes on Niijima island, Japan. Journal of Volcanology and Geothermal Research **29**, 71–98 (1986)
12. Lighthill, J.: A brief look back at the Review Meeting's Proceedings. In: Sir J. Lighthill (ed.) The Critical Review of VAN: Earthquake Prediction from Seismic Electric Signals, pp. 349–356. World Scientific, Singapore (1996)
13. Lighthill, J.: A brief look forward to future research needs. In: Sir J. Lighthill (ed.) The Critical Review of VAN: Earthquake Prediction from Seismic Electric Signals, pp. 373–376. World Scientific, Singapore (1996)
14. Masood, E.: Court charges open splite in Greek earthquake experts. Nature **377**, 375 (1995)
15. Masood, E.: Greek earthquake stirs controversy over claims for prediction method. Nature **375**, 617 (1995)
16. Monastersky, R.: Electric signals may herald earthquakes. Science News **148**, 260 (1995)
17. Nagao, T., Uyeda, S., Asai, Y., Kono, Y.: Anomalous changes in geoelectric potential preceding four earthquakes in Japan. In: Sir J.Lighthill (ed.) The Critical Review of VAN: Earthquake Prediction from Seismic Electric Signals, pp. 292–300. World Scientific, Singapore (1996)
18. Orihara, Y., Noda, Y., Nagao, T., Uyeda, S.: A possible case of SES selectivity at Kozu-shima island. J. Geodynamics **33**, 425–432 (2002)
19. Roumelioti, Z., Kiratzi, A., Benetatos, C.: The instability of M_w and M_L comparison for earthquakes in Greece for the period 1969 to 2007. Journal of Seismology **14**, 309–337 (2010)
20. Sarlis, N.V., Skordas, E.S., Lazaridou, M.S., Varotsos, P.A.: Investigation of the seismicity after the initiation of a Seismic Electric Signal activity until the main shock. arXiv:0802.3329v2 [cond-mat.stat-mech] (20 March 2008)
21. Sarlis, N.V., Skordas, E.S., Lazaridou, M.S., Varotsos, P.A.: Investigation of seismicity after the initiation of a Seismic Electric Signal activity until the main shock. Proc. Japan Acad., Ser. B **84**, 331–343 (2008)
22. Sarlis, N.V., Skordas, E.S., Lazaridou, M.S., Varotsos, P.A.: Investigation of the seismicity after the initiation of a Seismic Electric Signal activity until the main shock. arXiv:0802.3329v4 [cond-mat.stat-mech] (29 May 2008)
23. Scafetta, N., West, B.J.: Multiscaling comparative analysis of time series and a discussion on "earthquake conversations" in California. Phys. Rev. Lett. **92**, 138501 (2004)
24. Takahashi, I., Nagao, T., Uyeda, S.: On some geoelectric potential changes in Naha, Okinawa, Japan and their possible relationship with nearby earthquakes (in Japanese with English abstract). Bull. Inst. Oceanic Res. and Develop. **20**, 31–40 (1999)

25. Tsukui, M., Saito, K., Hayashi, K.: Frequent and intensive eruptions in the 9th century, Izu Islands, Japan: Revision of volcano- stratigraphy based on tephras and historical document (in Japanese with English abstract). Bull. Volcanol. Soc. Jpn. **51**, 327–338 (2006)
26. USGS: (2010). See the United States Geological Survey (USGS) earthquake search web page http://neic.usgs.gov/neis/epic/epic.html for the relevant seismic catalogs
27. Uyeda, S.: VAN method of short-term earthquake prediction shows promise. EOS Trans. AGU **79**, 573–580 (1998)
28. Uyeda, S., Al-Damegh, E., Dologlou, E., Nagao, T.: Some relationship between VAN Seismic Electric Signals (SES) and earthquake parameters. Tectonophysics **304**, 41–55 (1999)
29. Uyeda, S., Hayakawa, M., Nagao, T., Molchanov, O., Hattori, K., Orihara, Y., Gotoh, K., Akinaga, Y., Tanaka, H.: Electric and magnetic phenomena observed before the volcano-seismic activity in 2000 in the Izu Island Region, Japan. Proc. Natl. Acad. Sci. USA **99**, 7352–7355 (2002)
30. Uyeda, S., Kamogawa, M.: The prediction of two large earthquakes in Greece. EOS Trans. AGU **89**, 363 (2008)
31. Uyeda, S., Kamogawa, M.: Reply to a Comment on 'The prediction of two large earthquakes in Greece'. EOS Trans. AGU **91**, 163 (2010)
32. Uyeda, S., Kamogawa, M., Tanaka, H.: Analysis of electrical activity and seismicity in the natural time domain for the volcanic-seismic swarm activity in 2000 in the Izu Island region, Japan. J. Geophys. Res. **114**, B02310 (2009)
33. Uyeda, S., Nagao, T., Orihara, Y., Yamaguchi, T., Takahashi, I.: Geoelectric potential changes: Possible precursors to earthquakes in Japan. Proc. Natl. Acad. Sci. USA **97**, 4561–4566 (2000)
34. Uyeda, S., Nagao, T., Tanaka, H.: A report from the RIKEN international frontier research project on earthquakes. Terr. Atmos. Ocean. Sci. **15**, 269–310 (2004)
35. Varotsos, P.: The Physics of Seismic Electric Signals. TERRAPUB, Tokyo (2005)
36. Varotsos, P., Alexopoulos, K., Lazaridou, M.: Latest aspects of earthquake prediction in Greece based on Seismic Electric Signals, II. Tectonophysics **224**, 1–37 (1993)
37. Varotsos, P., Eftaxias, K., Lazaridou, M., Nomicos, K., Sarlis, N., Bogris, N., Makris, J., Antonopoulos, G., Kopanas, J.: Recent earthquake prediction results in Greece based on the observation of Seismic Electric Signals. Acta Geophys. Pol. **44**, 301–327 (1996)
38. Varotsos, P., Lazaridou, M.: Latest aspects of earthquake prediction in Greece based on Seismic Electric Signals. Tectonophysics **188**, 321–347 (1991)
39. Varotsos, P., Lazaridou, M., Eftaxias, K., Antonopoulos, G., Makris, J., Kopanas, J.: Short term earthquake prediction in Greece by Seismic Electric Signals. In: Sir J. Lighthill (ed.) The Critical Review of VAN: Earthquake Prediction from Seismic Electric Signals, pp. 29–76. World Scientific, Singapore (1996)
40. Varotsos, P., Sarlis, N., Bogris, N., Makris, J., Kapiris, P., Abdulla, A.: A comment on the ΔV/L-criterion for the identification of Seismic Electric Signals, pp. 1–45. TERRAPUB, Tokyo (1999)
41. Varotsos, P., Sarlis, N., Skordas, E.: A note on the spatial extent of the Volos SES sensitive site. Acta Geophys. Pol. **49**, 425–435 (2001)
42. Varotsos, P.A.: Recent Seismic Electric Signals (SES) activities in Greece. Acta Geophys. Pol. **54**, 158–164 (2006)
43. Varotsos, P.A.: What happened before the last five strong earthquakes in Greece. Proc. Jpn. Acad., Ser. B: Phys. Biol. Sci. **82**, 86–91 (2006)
44. Varotsos, P.A., Sarlis, N.V., Skordas, E.S.: Seismic Electric Signals and $1/f$ "noise" in natural time. arXiv:0711.3766v3 [cond-mat.stat-mech] (1 February 2008)
45. Varotsos, P.A., Sarlis, N.V., Skordas, E.S.: Spatio-temporal complexity aspects on the interrelation between Seismic Electric Signals and seismicity. Practica of Athens Academy **76**, 294–321 (2001)
46. Varotsos, P.A., Sarlis, N.V., Skordas, E.S.: Seismic Electric Signals and seismicity: On a tentative interrelation between their spectral content. Acta Geophys. Pol. **50**, 337–354 (2002)
47. Varotsos, P.A., Sarlis, N.V., Skordas, E.S.: Detrended fluctuation analysis of the magnetic and electric field variations that precede rupture. CHAOS **19**, 023114 (2009)
48. Varotsos, P.A., Sarlis, N.V., Skordas, E.S., Lazaridou, M.S.: Fluctuations, under time reversal, of the natural time and the entropy distinguish similar looking electric signals of different dynamics. J. Appl. Phys. **103**, 014906 (2008)

49. Varotsos, P.A., Sarlis, N.V., Skordas, E.S., Tanaka, H.K., Lazaridou, M.S.: See (the freely available) EPAPS Document No. E-PLEEE8-74-190608 originally from P.A. Varotsos, N.V. Sarlis, E.S. Skordas, H.K. Tanaka and M.S. Lazaridou *Phys. Rev. E* **74**, 021123 (2006). For more information on EPAPS, see http://www.aip.org/pubservs/epaps.html.
50. Varotsos, P.A., Sarlis, N.V., Skordas, E.S., Tanaka, H.K., Lazaridou, M.S.: Attempt to distinguish long-range temporal correlations from the statistics of the increments by natural time analysis. Phys. Rev. E **74**, 021123 (2006)
51. Varotsos, P.A., Sarlis, N.V., Skordas, E.S., Tanaka, H.K., Lazaridou, M.S.: Entropy of seismic electric signals: Analysis in the natural time under time reversal. Phys. Rev. E **73**, 031114 (2006)
52. Varotsos, P.A., Sarlis, N.V., Skordas, E.S., Tanala, H.K., Lazaridou, M.S.: Additional evidence on some relationship between Seismic Electric Signals and earthquake source parameters. Acta Geophys. Pol. **53**, 293–298 (2005)
53. Varotsos, P.A., Sarlis, N.V., Skordas, E.S., Uyeda, S., Kamogawa, M.: Natural time analysis of critical phenomena. the case of seismicity. EPL **92**, 29002 (2010)
54. Varotsos, P.A., Sarlis, N.V., Tanaka, H.K., Skordas, E.S.: Similarity of fluctuations in correlated systems: The case of seismicity. Phys. Rev. E **72**, 041103 (2005)
55. Varotsos, P.A., Sarlis, N.V., Tanaka, H.K., Skordas, E.S.: Some properties of the entropy in the natural time. Phys. Rev. E **71**, 032102 (2005)
56. Varotsos, P.A., Sarlis, N.V., Skordas, E.S.: Electric fields that "arrive" before the time derivative of the magnetic field prior to major earthquakes. Phys. Rev. Lett. **91**, 148501 (2003)